REPORT DOCUMENTATION PAGE

Form Approved
OMB No. 0704-0188

1. REPORT DATE *(DD-MM-YYYY)*: 04-06-2003

2. REPORT TYPE: Technical Presentation

3. DATES COVERED *(From - To)*:

4. TITLE AND SUBTITLE

Usage of Fiber Grating Strain Sensors for Diagnostics of Composite Pressure Vessels

5a. CONTRACT NUMBER: **F04611-02-C-0007**

5b. GRANT NUMBER:

5c. PROGRAM ELEMENT NUMBER:

5d. PROJECT NUMBER: **3005**

5e. TASK NUMBER: **02AG**

5f. WORK UNIT NUMBER:

6. AUTHOR(S)

E. Udd, M. Kunzler, S. Calvert, S. Kreger (Blue Road Research); M. Johnson, K. Mildenhall (ATK Thiokol Propulsion)

7. PERFORMING ORGANIZATION NAME(S) AND ADDRESS(ES)

Blue Road Research
376 NE 219th Avenue
Gresham OR 97030

8. PERFORMING ORGANIZATION REPORT NUMBER:

9. SPONSORING / MONITORING AGENCY NAME(S) AND ADDRESS(ES)

Air Force Research Laboratory (AFMC)
AFRL/PRS
5 Pollux Drive
Edwards AFB CA 93524-7048

10. SPONSOR/MONITOR'S ACRONYM(S):

11. SPONSOR/MONITOR'S NUMBER(S): **AFRL-PR-ED-VG-2003-148**

12. DISTRIBUTION / AVAILABILITY STATEMENT

Approved for public release; distribution unlimited.

13. SUPPLEMENTARY NOTES

For presentation at the 16th International Conference on Optical Fiber Sensors in Nara, Japan, taking place 13-17 October 2003.

14. ABSTRACT

20030812 207

15. SUBJECT TERMS

16. SECURITY CLASSIFICATION OF:			17. LIMITATION OF ABSTRACT	18. NUMBER OF PAGES	19a. NAME OF RESPONSIBLE PERSON
					Leilani Richardson
a. REPORT	b. ABSTRACT	c. THIS PAGE			19b. TELEPHONE NUMBER *(include area code)*
Unclassified	Unclassified	Unclassified	A	39	(661) 275-5015

Standard Form 298 (Rev. 8-98)
Prescribed by ANSI Std. 239.18

USAGE OF FIBER GRATING STRAIN SENSORS FOR DIAGNOSTICS OF COMPOSITE PRESSURE VESSELS

E. Udd, M. Kunzler, S. Calvert, and S. Kreger
Blue Road Research
376 NE 219th Avenue, Gresham, Oregon 97030

M. Johnson and K. Mildenhall
ATK Thiokol Propulsion
Brigham City, Utah 84302

ABSTRACT

Single and multi-dimensional fiber grating strain sensors have been embedded into a composite pressure vessel and used to determine the presence of damage associated with a cut tow and a Teflon tape defect.

MULTI-AXIS FIBER GRATING STRAIN SENSORS

Figure 1(a) illustrates a multi-axis grating written onto polarization preserving fiber, which is subject to uniform transverse loading. In this case, the two spectral reflection peaks, corresponding to the effective fiber gratings along each birefringent (polarization) axis, will move apart or together uniformly providing a means to measure transverse strain.[1,2,3] In the case where load along the transverse axis is not uniform, as shown in Figure 1(b), the peak associated with the nonuniform transverse load will split.[1] The transverse strain gradient can be measured quantitatively by the spectral separation between the peaks. The portion of the grating under a fixed transverse load is reflected in the amplitude of the peak. For example, in Figure 1(a) the transverse load along the vertical axis is uniform. There are only two spectral peaks as a result, and their spectral separation defines the transverse load. In the case of Figure 1(b), the transverse load has two values along the vertical axis, each along approximately one half of the fiber grating length. In this case, the spectral peak corresponding to the vertical axis splits. The spectral shift between these subpeaks determines the transverse load gradient. As an example, a shift of 0.1 nm would correspond to approximately 300 microstrain. The amplitudes of the two split peaks are approximately equal indicating that each of the two distinct transverse load regions are approximately equal (the amplitude of the fiber grating spectral peak indicates the fraction of the fiber grating under that load). The response of the fiber to transverse strain is approximately 1/3 of that of axial strain along the length of the fiber. As a specific example at 1300 nm, a spectral shift of 0.01 nm along the fiber axis corresponds to 10 microstrain. A peak-to-peak separation of 0.01 nm due to nonuniform transverse strain corresponds to approximately 30 microstrain for 125 micron diameter bow-tie polarization preserving fiber. These properties may be used effectively to measure the extent and location of damage in a composite pressure vessel.

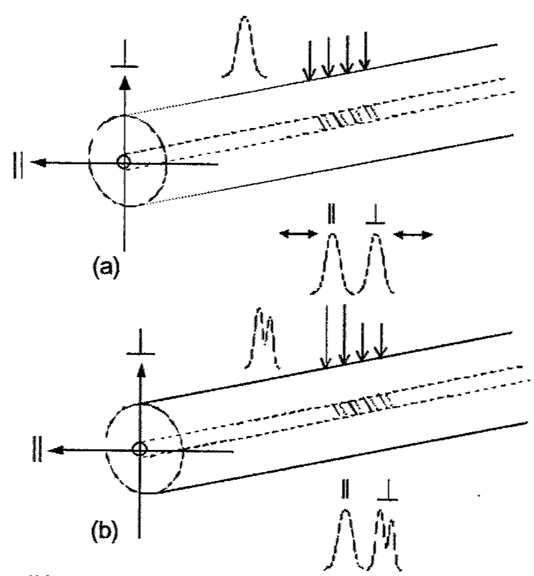

Figure 1. The Effect of Strain on a Multi-Axis Fiber Grating (a) When a multi-axis fiber grating sensor is subject to uniform transverse loadi ng two spectral reflections result whose spectral separation is a measure of transverse strain. (b) When transverse strain across the fiber is not uniform along one of the birefringent (polarization) axes, the peak associated with that axis splits, providng a means to measure transverse strain gradients effectively and quantitatively.

Usage of Multi-axis Fiber Grating Strain Sensors to Detect Damage in a Composite Pressure Vessel

A pressure vessel was fabricated and multi-axis and single axis fiber grating strain sensors were placed to enable the detection of damage. The transverse strain axes of the multi-axis fiber grating sensors were aligned in the plane and out of the plane of the cylinder. Damage was purposefully introduced into two locations prior to cure. In the first damage area, a section of prepreg tow was cut. In the second damage area, a piece of Teflon tape was introduced. The dual-axis fiber grating sensor in the area of the cut tow was able to clearly indicate that damage occurred in the plane of the cylinder after cure. In the case of the Teflon tape, the dual-axis sensor in the vicinity did not detect damage after cure, but it was able to pick up damage after the first pressure cycle. Impacts were made on the composite pressure vessel on both the cut tow and Teflon tape damage area with resulting changes in the multi-axis strain fields that could be observed after each impact, and with additional changes induced by subsequent pressure cycling.

Figure 2(a) shows an overview of the part in the process of being fabricated. Figure 2(b) shows the placement and orientation of a single and dual-axis fiber grating strain sensor. Figure 2(c) shows the placement of a Teflon tape defect relative to the fiber grating strain sensors in this location.

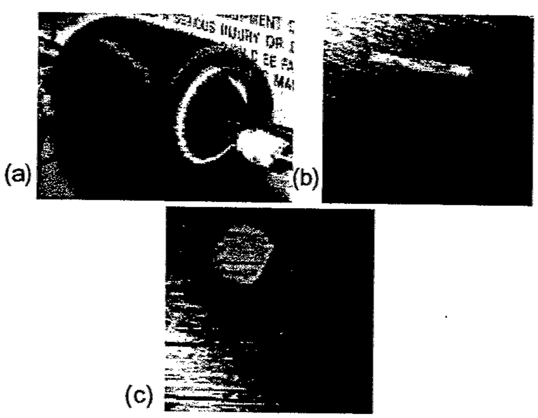

Figure 2. Fabrication of Composite Pressure Vessel (a) Part, (b) placement of dual-axis fiber grating strain sensor in prepreg tow on the first helical winding and a bare single axis fiber grating strain sensor orthogonal to it, (c) introduction of Teflon tape defect near the single and dual-axis fiber grating strain sensor.

Figure 3 shows the spectral profile of the dual-axis fiber grating strain sensor placed near the area of the cut tow damage site in the pressure vessel. In this case, prepreg tow alignment elements were placed on either side of the fiber grating but not over it, so the dual-axis fiber grating was integrated directly into the composite part. Before cure and completion of the composite pressure vessel, the two spectral peaks corresponding to the two transverse axes of the dual-axis fiber grating strain sensor are undistorted by transverse strain gradients. The short wavelength peak is aligned in the plane of the cylinder while the long wavelength peak is orthogonal to it. After the cure, significant transverse strain gradients appear on the short wavelength peak corresponding to transverse strain gradients in the plane of the cylinder, in the direction of the cut tow. Of the six dual-axis fiber grating strain sensors placed in the part this was the only one exhibiting this type of behavior.

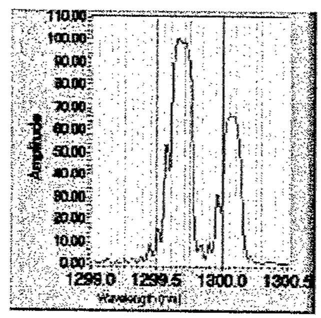

(a)

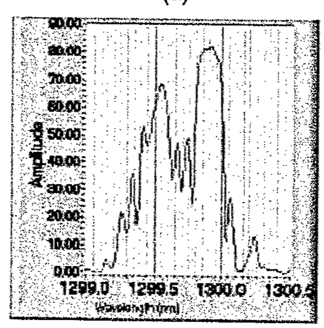

(b)

Figure 3. Aligned Dual-Axis Fiber Grating Strain Sensor Placed Bare into the Composite Pressure Vessel Near the Area of the Cut Tow Damage Site (a) Before cure and (b) after cure.

Figure 4 shows a sequence illustrating transverse strain gradients on a single axis fiber grating strain sensor near the Teflon tape defect through the first pressure cycle.

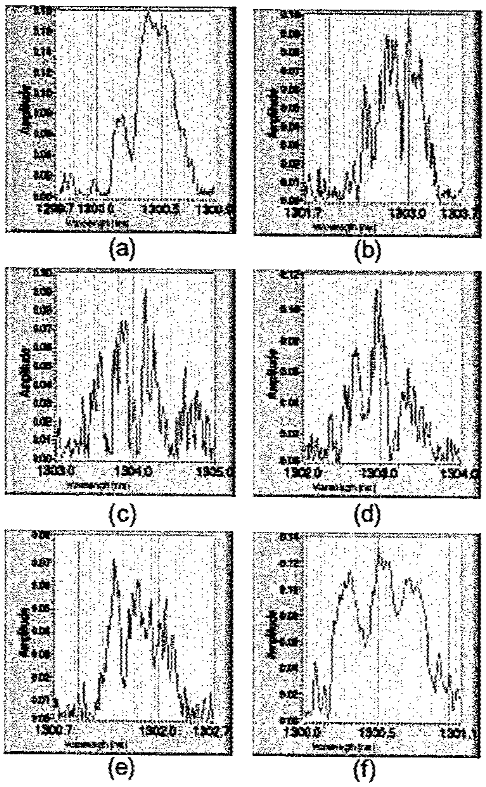

Figure 4. Sequence of Spectral Profiles
Sequence of spectral profiles from single axis fiber grating strain sensor placed bare into the part approximately 2.5 cm from the Teflon tape damage site during the first pressure cycle (a) 0 psi, (b) 666 psi, (c) 1000 psi, (d) 666 psi, (e) 333 psi, and (f) return to 0 psi

The advantage of using multi-axis sensors is that the directions of the transverse strain gradients, as well as the magnitudes are known. In the case of the damage sequence involving the cut tow of Figure 3 the know orientation of the multi-axis fiber grating sensor allows the user to understand that damage is in the plane of the cylinder of the composite pressure vessel. In addition, from Figure 3 it is apparent that out of the plane of the cylinder the spectral peak associated with that direction shows no change indicating that in this direction damage did not occur. By using arrays of multi-axis fiber grating sensors the directional information may be used to localize and characterize the extent of damage. In the case of Figure 4, the single axis fiber grating sensor located near the Teflon tape defect severe transverse strain gradients arise and the evolution of damage throughout the pressure cycle is clearly evident.

These transverse strain gradients are locked in after the cycle is complete. Because the fiber grating is single axis the direction of the damage is not known and information for both out of plane and in plane transverse, strain gradients as well as possible axial strain gradients are intermixed. When the damage sites around the cut tow area of Figure 3 and the Teflon tape area of Figure 4 are impacted the resulting damage releases the transverse strain gradients and eventually the fiber grating spectral profiles move back to their unloaded state.

SUMMARY

The ability of single and multi-axis fiber grating strain sensors to detect cut tow and Teflon tape defects in a composite pressure vessel have been shown. The multi-axis fiber grating strain sensors have the ability to indicate the direction of damage. Additional work is being pursued to refine and extend the ability of multi-axis fiber grating strain sensor arrays to accurately measure and localize damage in composite parts.

ACKNOWLEDGEMENTS

This work was supported under the Phase I SBIR contract to Blue Road Research, F04611-01-C-0038, granted by Edwards AFB. Dr. Gregory Ruderman is the Technical Program Monitor. Blue Road Research gratefully acknowledges the support of this SBIR and Dr. Ruderman.

REFERENCES

1.Perez, I., H.L. Cui, and E. Udd, "Acoustic Emission Detection using Fiber Bragg Gratings", *Proceedings of SPIE*, **Vol 4328**, 2001 pp. 209

2. Udd, Eric, W.L. Schulz, J.M. Seim, E. Haugse, A. Trego, P.E. Johnson, T.E. Bennett, D.V. Nelson, and A. Makino, "Multidimensional Strain Field Measurements using Fiber Optic Grating Sensors", *Proceedings of SPIE,* **Vol. 3986**, 2000 pp. 254

3. Schulz, Whitten, E. Udd, J.M. Seim, A. Trego, and I.M. Perez, "Progress on Monitoring of Adhesive Joints using Multiaxis Fiber Grating Sensors", *Proceedings of SPIE*, **Vol. 3991**, 2000 pp. 52

BLUE ROAD RESEARCH

Usage of Fiber Grating Strain Sensors for Diagnostics of Composite Pressure Vessels

16th International Conference on Optical Fiber Sensors (OFS-16)
October 13-17, 2003
Nara, Japan

E. Udd, M. Kunzler, S. Calvert, and S. Kreger
Blue Road Research

M. Johnson and K. Mildenhall
ATK Thiokol Propulsion

Acknowledgments

This work was supported under two SBIR contracts to Blue Road Research, The adhesive joint instrumentation portion of this work was supported in part by the US NAVY contract N68335-98-C-0122. Dr. Ignacio Perez, Technical Program Monitor, and “Fiber Grating Sensor System to Determine Motor Case Damage”, F04611-01-C-0038, Dr. Gregory Ruderman, Technical Program Monitor.

Blue Road Research gratefully acknowledges the support of these SBIRs, Dr. Perez and Dr. Ruderman.

BLUE ROAD RESEARCH

Fiber Optic Sensor Advantages

- Lightweight / nonobtrusive
- Passive / low power
- EMI resistant
- High sensitivity and bandwidth
- Large multiplexing potential
- Environmental ruggedness
- Complementary to telecom / optoelectronics

Unique Technologies

- Multiaxis Fiber Grating Sensors
- Transverse and Shear Strain Measurements
- High Speed Sensors/Systems (up to 10 MHz)
- Pressure, Corrosion, Environmental Sensing with very low temperature sensitivity, high multiplexing potential

BLUE ROAD RESEARCH

Transmission and Reflection Spectra from Fiber Bragg Grating

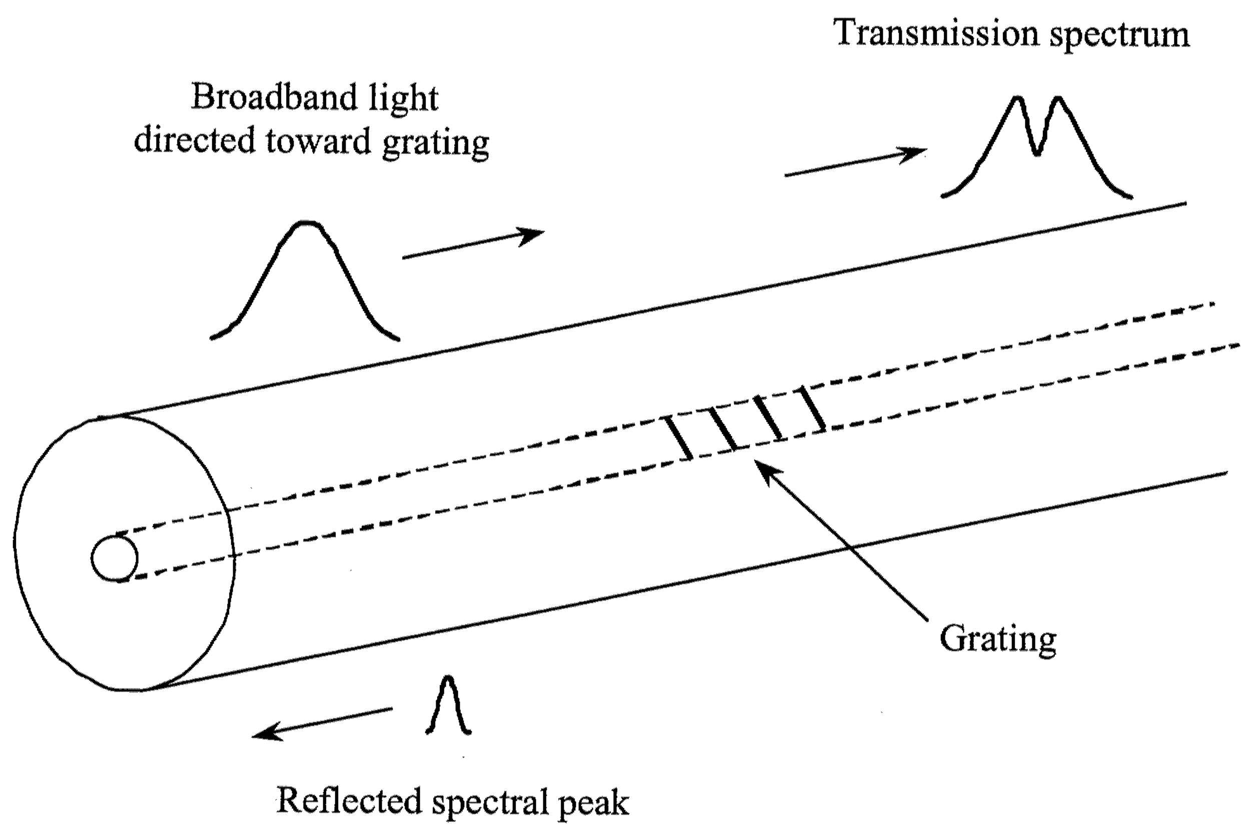

BLUE ROAD RESEARCH

Uniform Transverse Loading

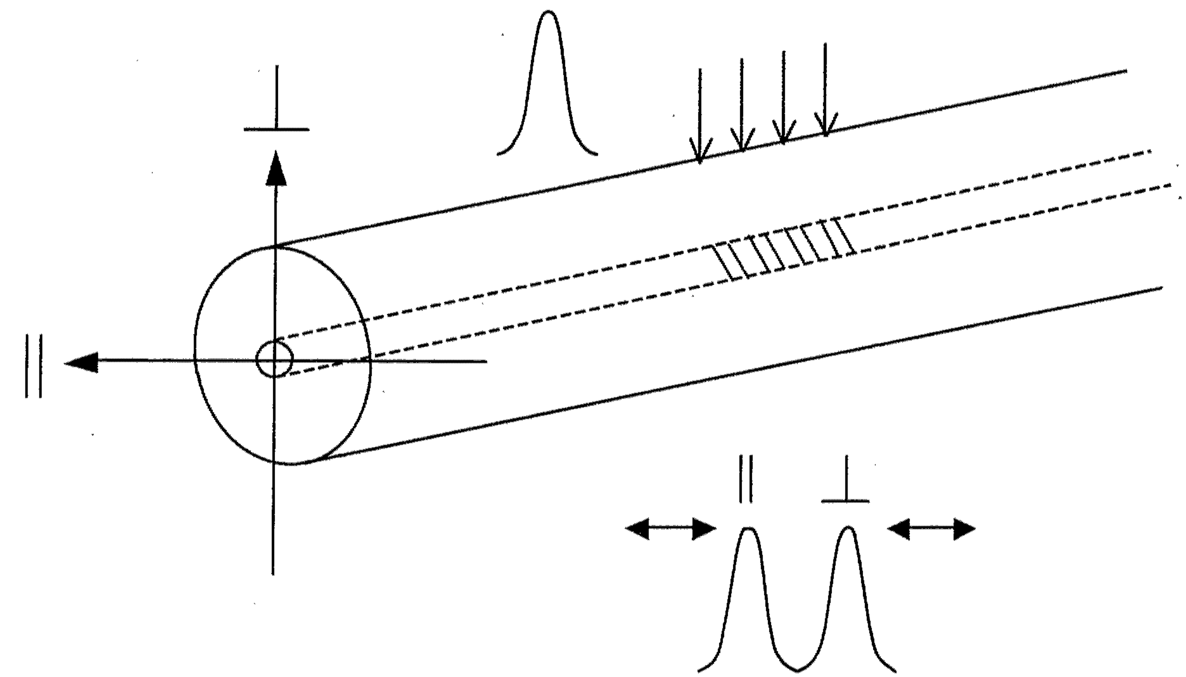

Axial Loading

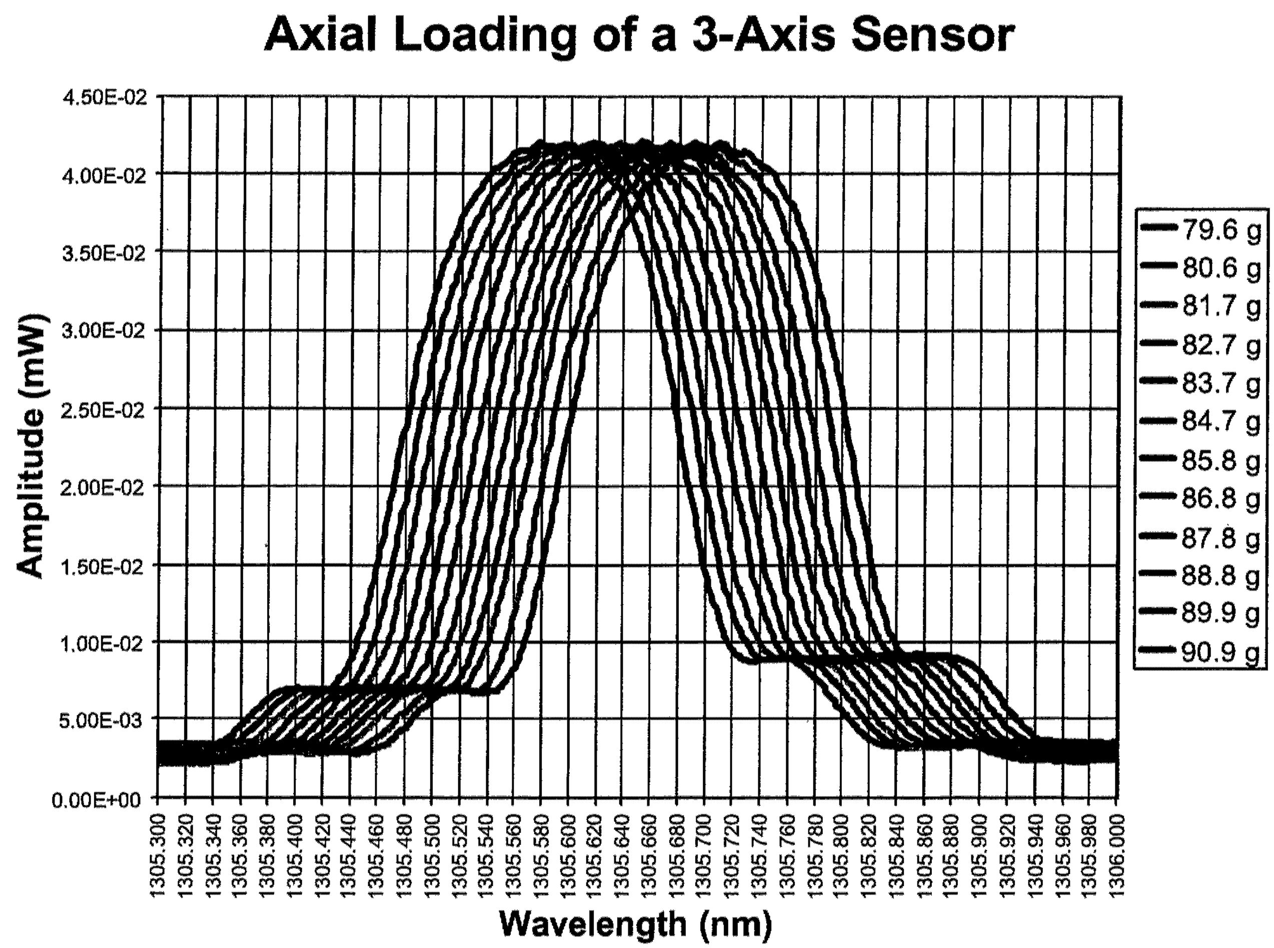

BLUE ROAD RESEARCH

Transverse Loading

Transverse Loading of a 3-Axis Sensor

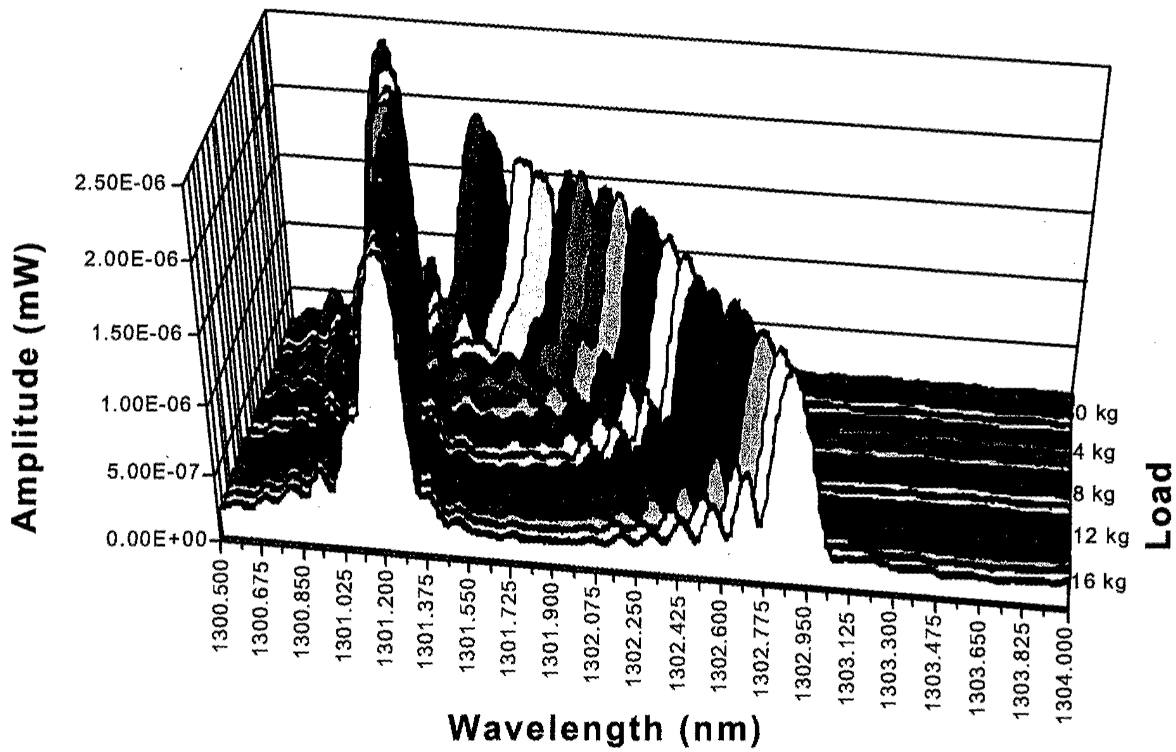

BLUE ROAD RESEARCH

Transverse Strain Gradients

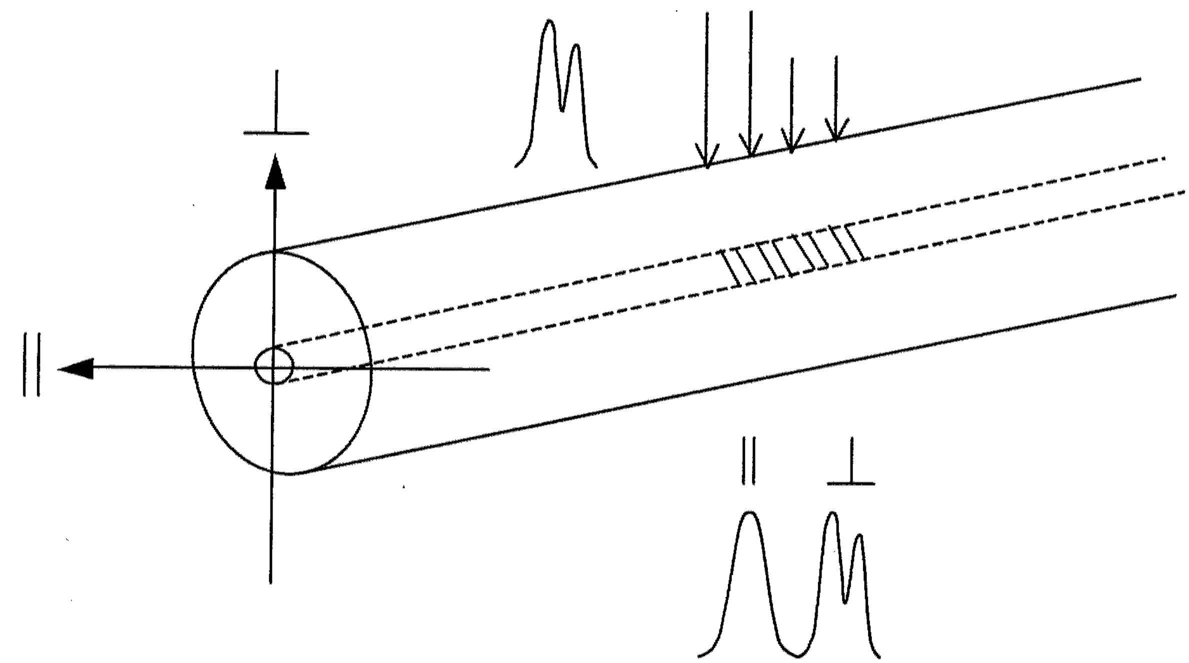

Joint Health Monitoring System

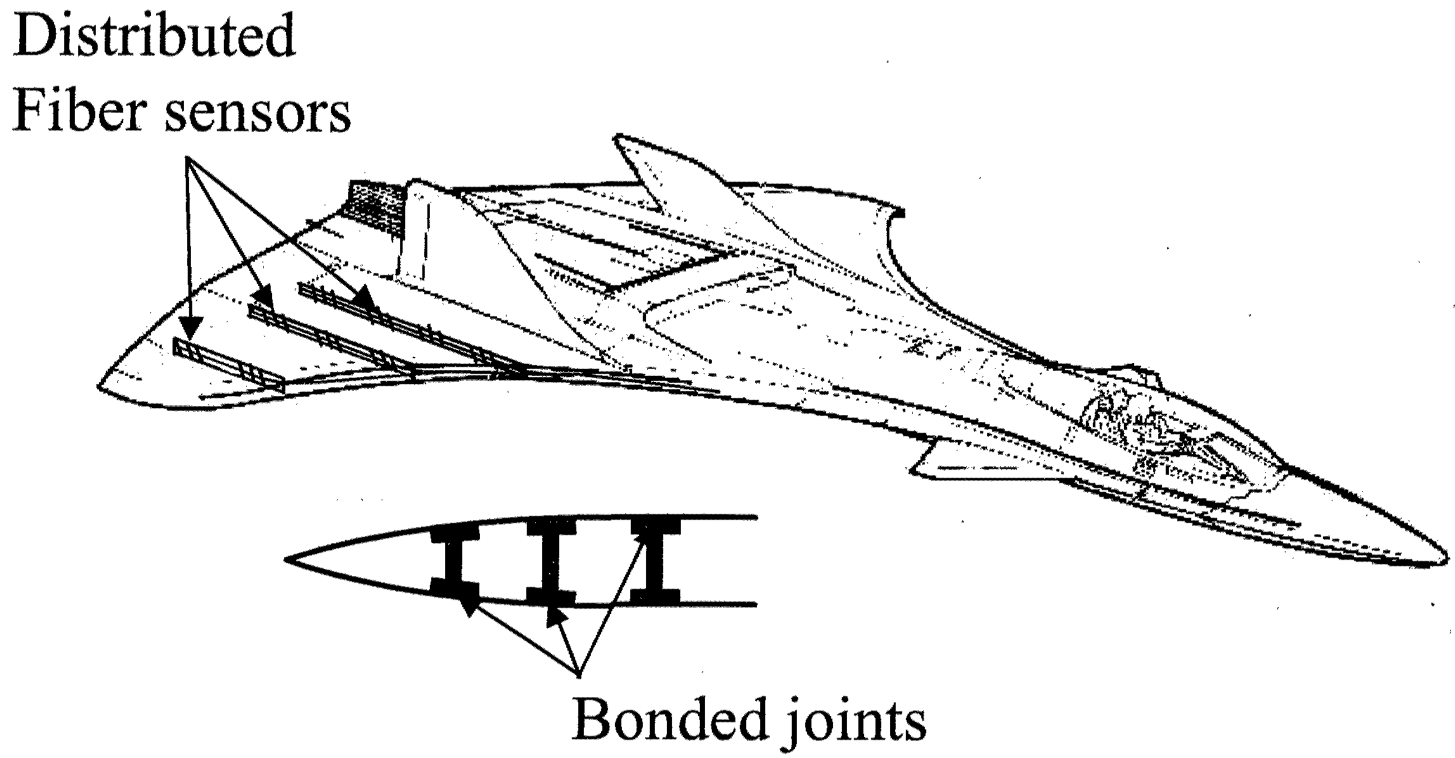

Instrumented Joint

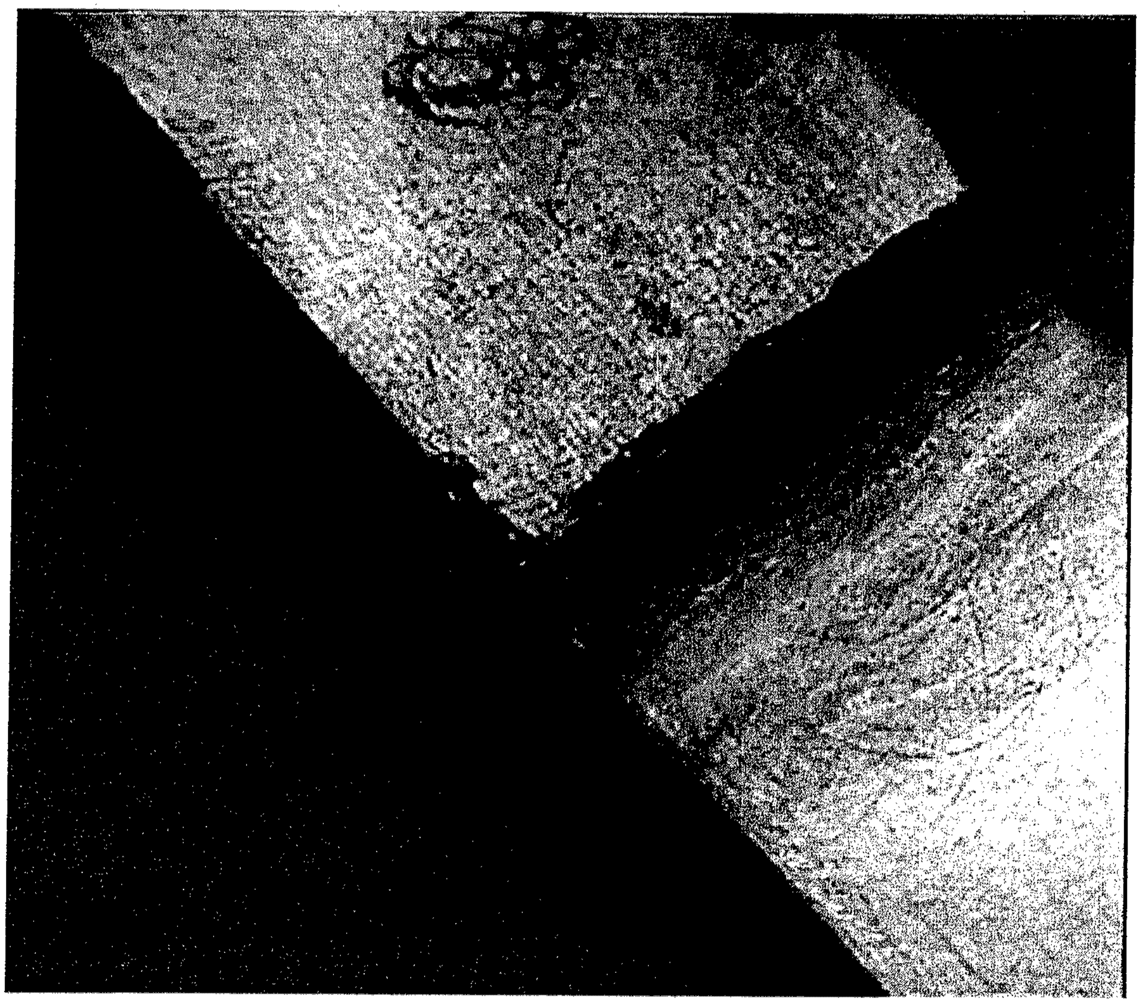

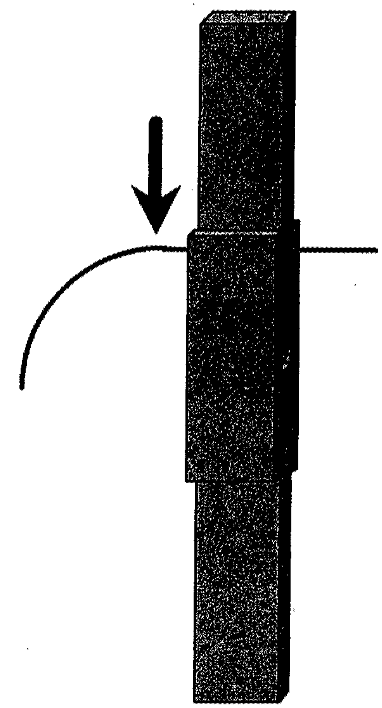

Shear Strain Measurement in Adhesive Joint

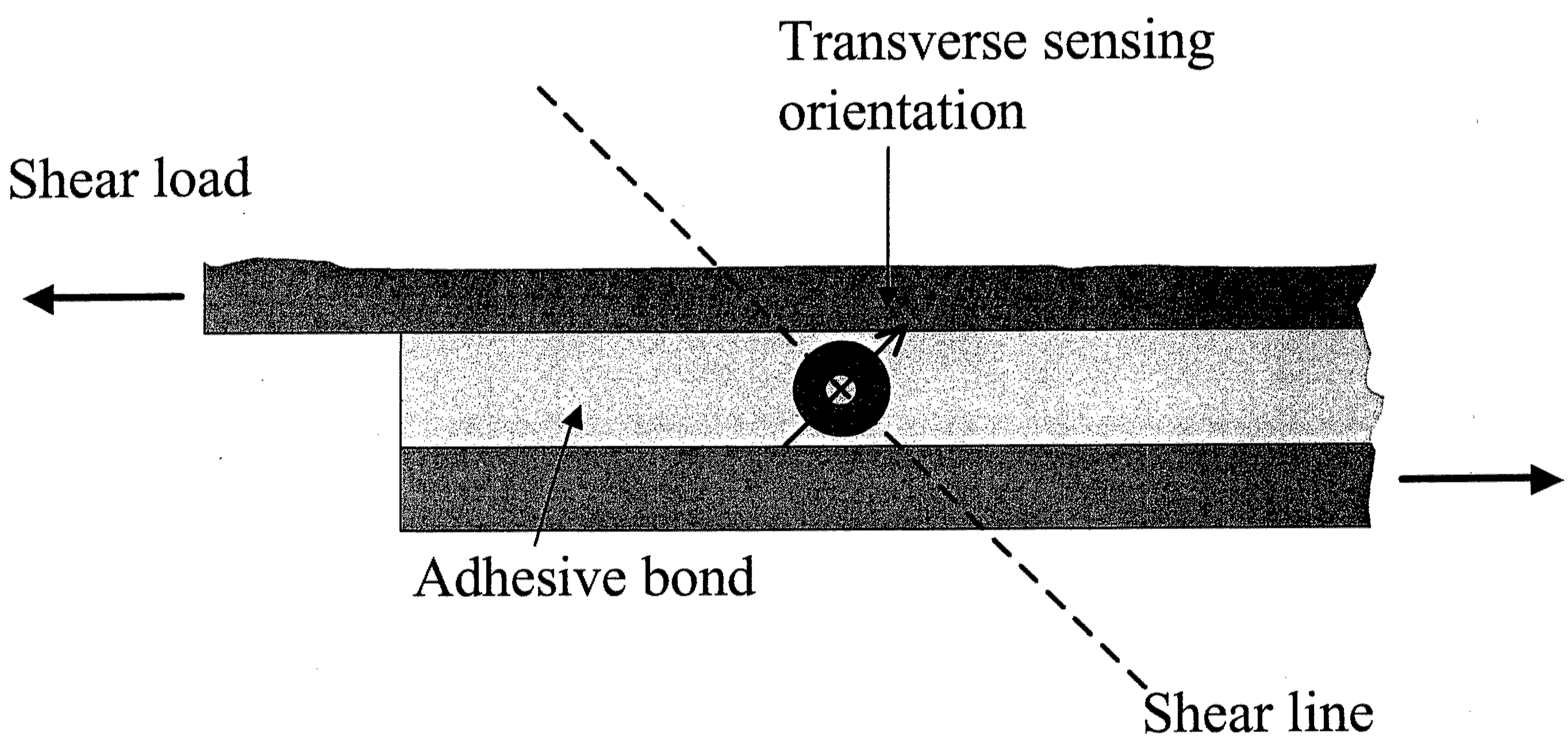

Sensors embedded in, and Retro-fitted to, an Adhesive Joint

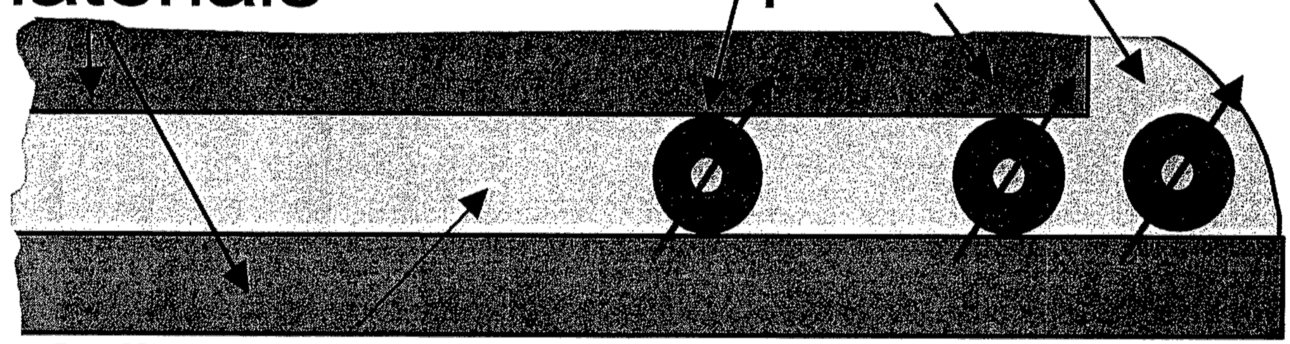

Retrofit Spectral Data

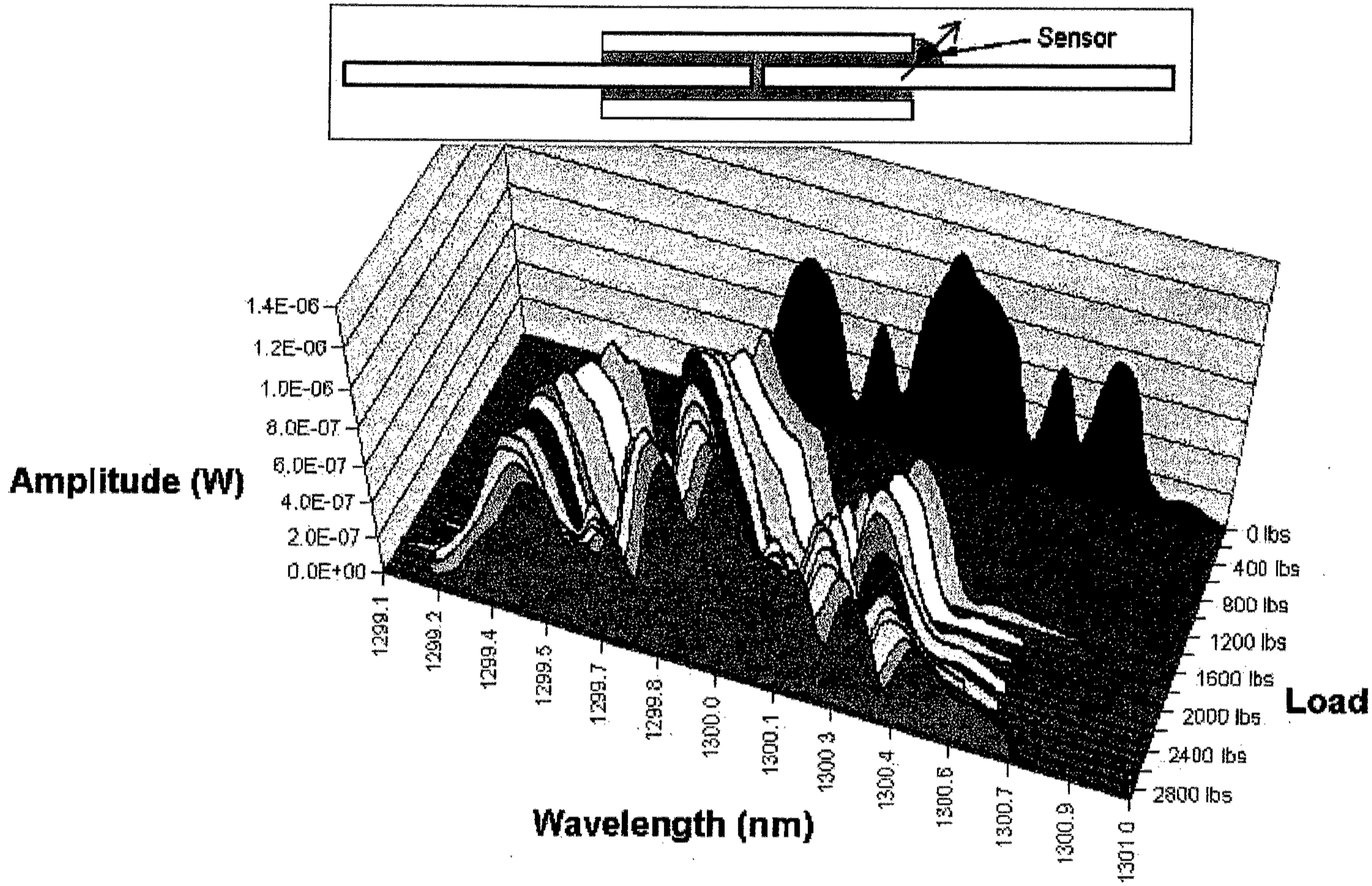

BLUE ROAD RESEARCH

Adhesive Joint Summary

- Embedded Sensors can Measure Shear Strain when the Transverse Sensing axes are Aligned with the Shear Direction

- No reduction in Part Integrity

- The Multiaxis Sensors can be Retrofit to Existing Joints and Provide Strain Information

- Strain Information from Sensors can be used to Identify the State of the Part and Predict Joint Failure.

Casing with Embedded Fiber Grating Strain Sensors

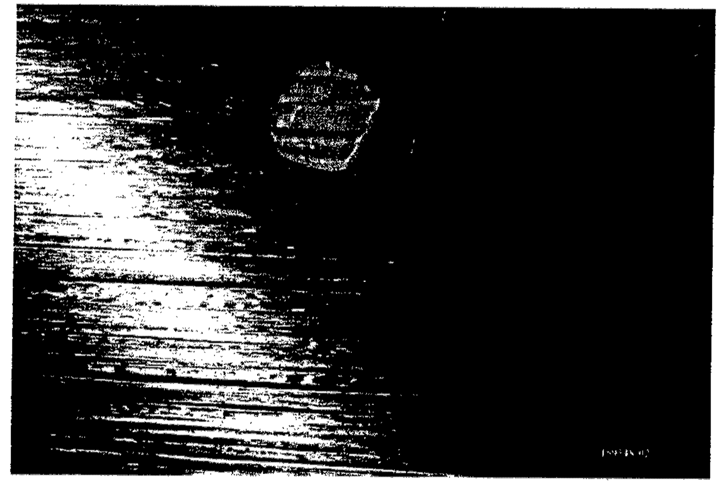

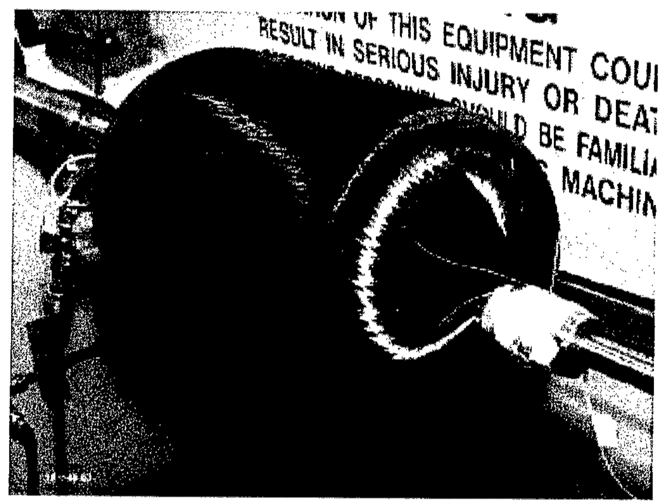

BLUE ROAD RESEARCH

Casing Cylinder Parameters

Parameter	Characteristics
Composite	T700/UF3369
Liner	Approx. 12" dia. & 20" length Cross linked Polyethylene 5.7 lbs. Made by Roto Molding of Utah
Winding Plan: Wind directly over plastic liner	3 Helical layers (0.0705 in. thick) 2 to boss -10 deg. X 1stepped back one bandwidth -16 deg. Xsb 7 hoop plies (0.0823 in. thick) 4 tows/band 5 lbs/tow tension
Winding Sequence	X O O O Xsb O O O X O

Apply internal pressure to mandrel during winding and cure.

BLUE ROAD RESEARCH

The Relative Position of Sensors #1 and #2, Which Were Placed After the First Helical Winding

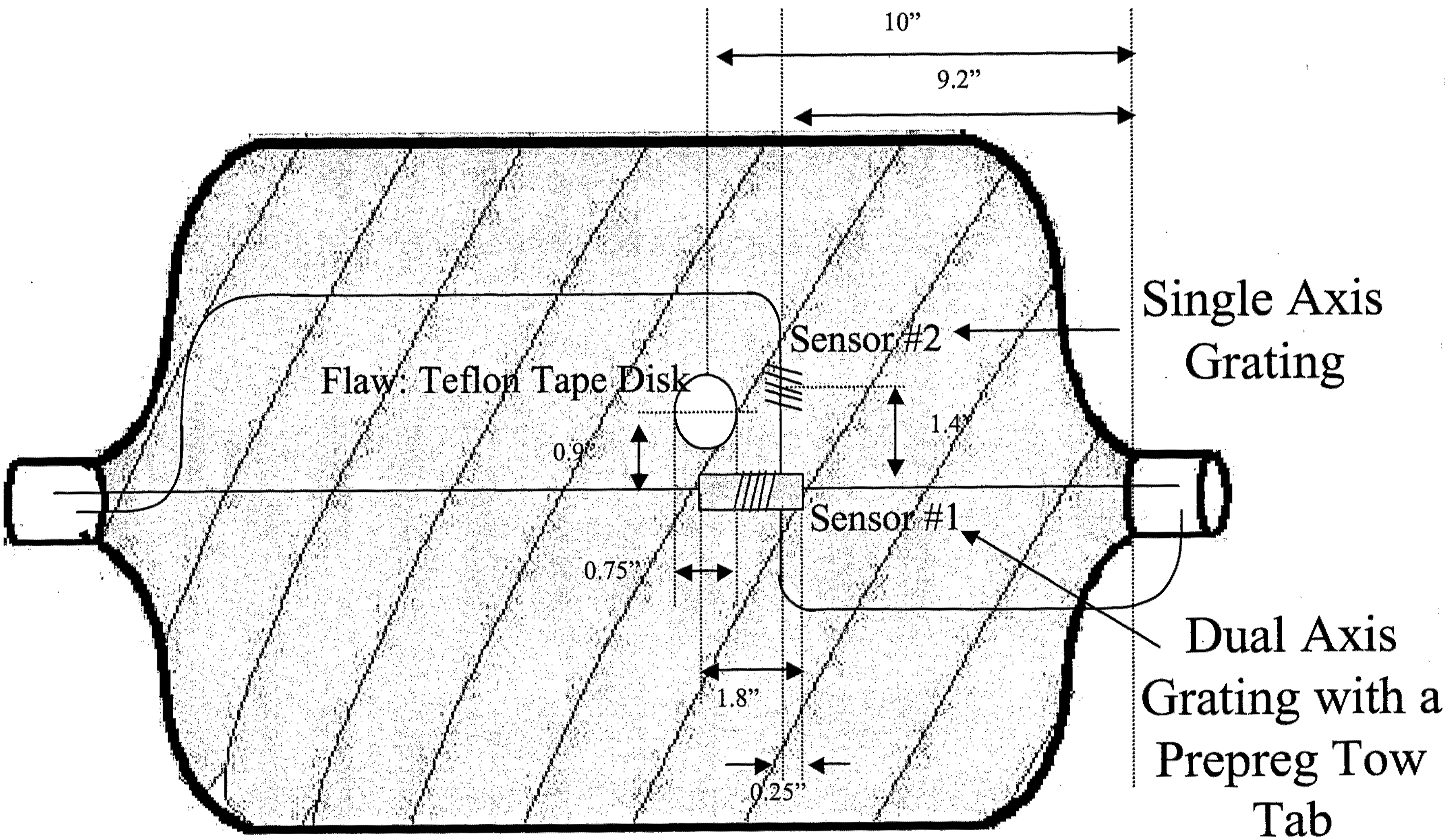

BLUE ROAD RESEARCH

Distances Between Adjacent Sensors

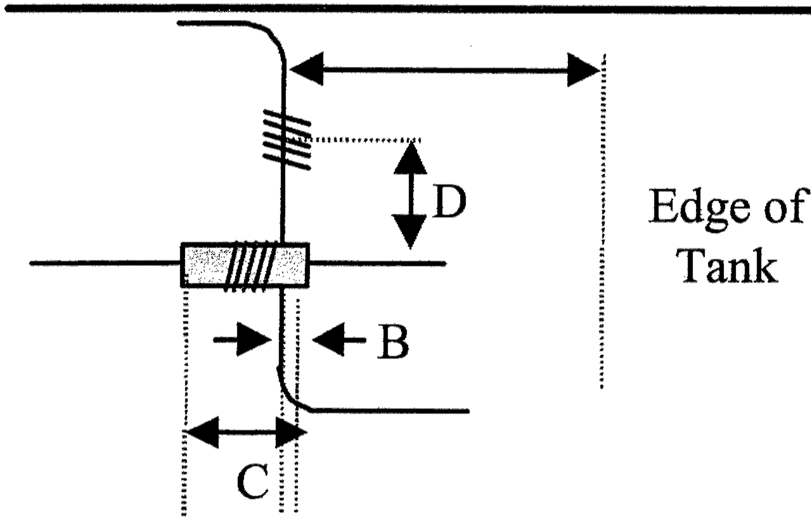

Sensor Numbers[a]	A (in.)	B (in.)	C (in.)	D (in.)
1 and 2	9.2	0.25	1.8	1.4
3 and 4	9	0.2	1.75	1.2
5 and 6	9.8	0.125	1.75	1.25
11and 12	9.5	*	*	1.75

* Not Recorded

[a] Dual Axis: Sensor #1, 4, 6 and 12
Single Axis: Sensor #2, 3, 5, and 11

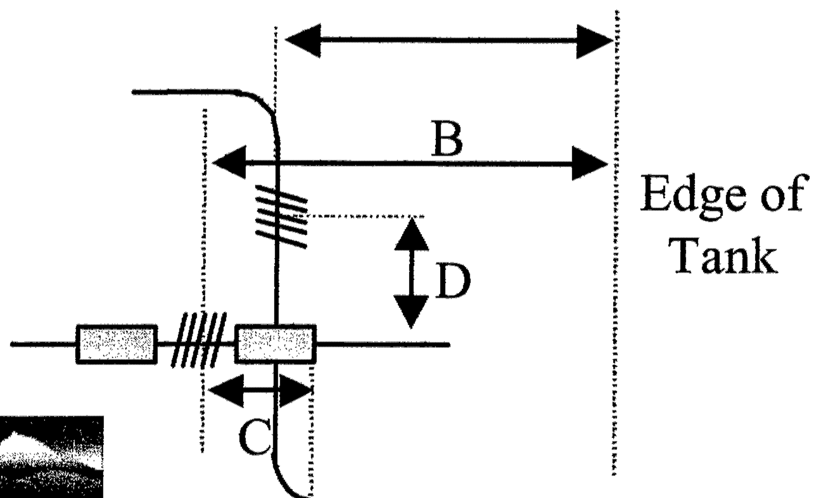

Sensor Numbers[a]	A (in.)	B (in.)	C (in.)	D (in.)
7 and 8 [b]	9.75	11	1.4	1.75
9 and 10	9.75	11.5	2	2

[a] Dual Axis: Sensor #8 and #10
Single Axis: Sensor #7 and #9

[b] Flaw: Cut 1 Band in the Subsequent Layer

BLUE ROAD RESEARCH

Phase I Demonstration Article Placed in the Pressure Test Chamber

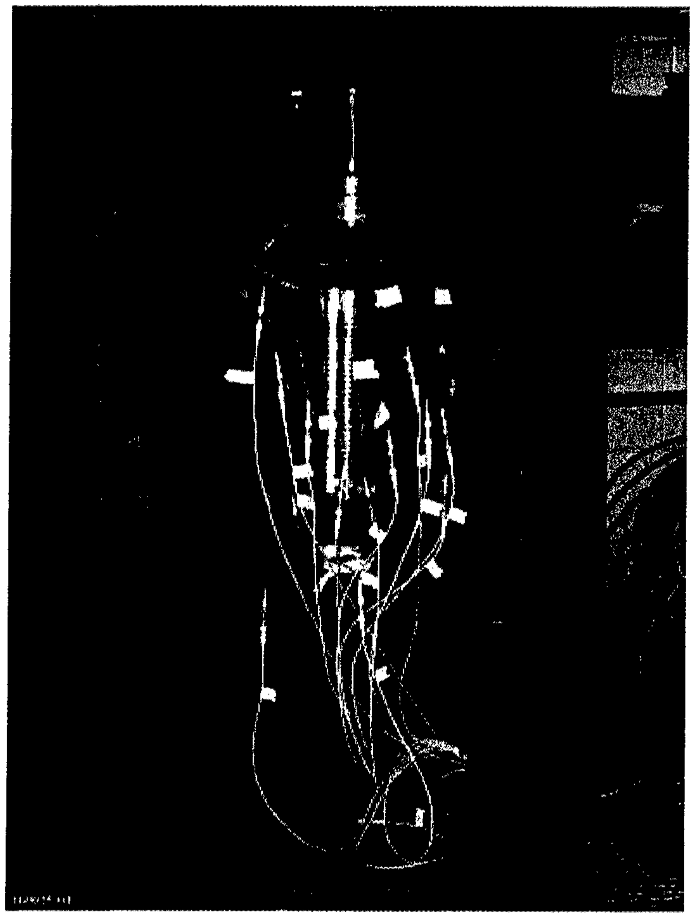

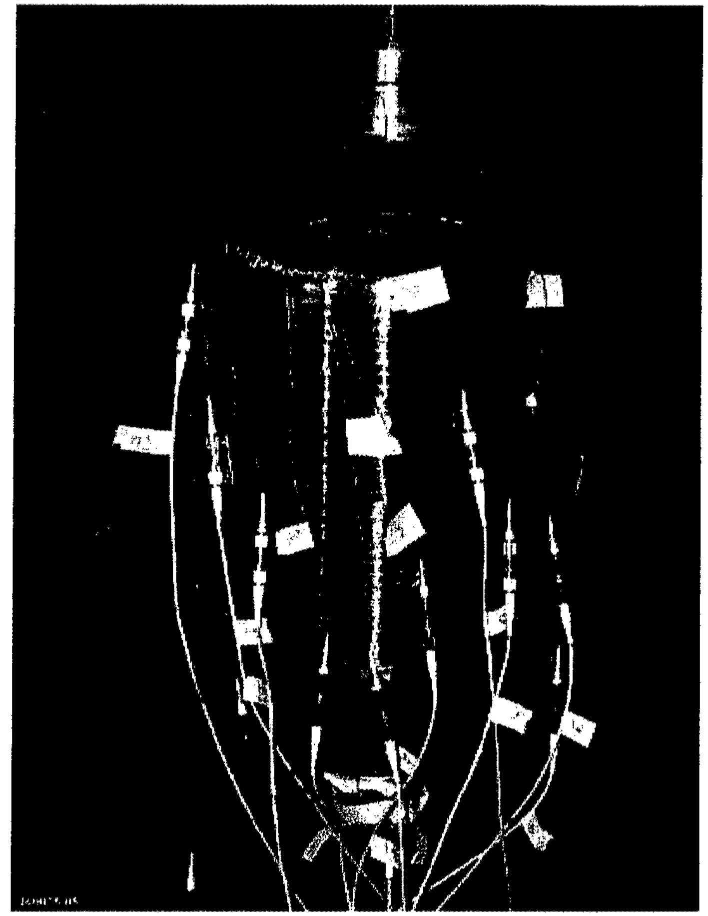

Spectral Profile of Sensor #2 (a) before and (b) after curing process

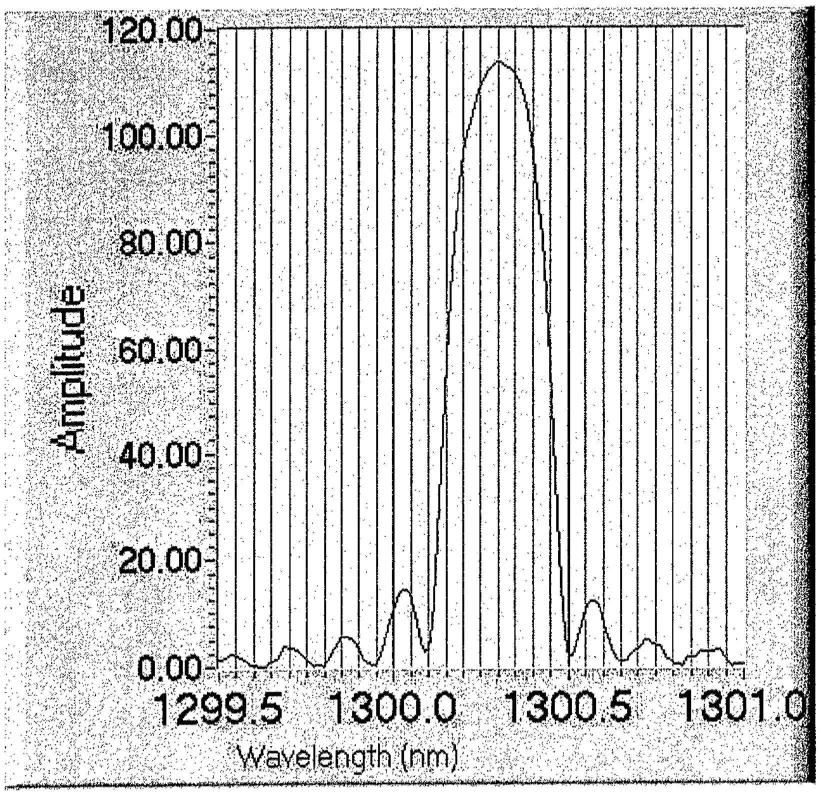

(a)

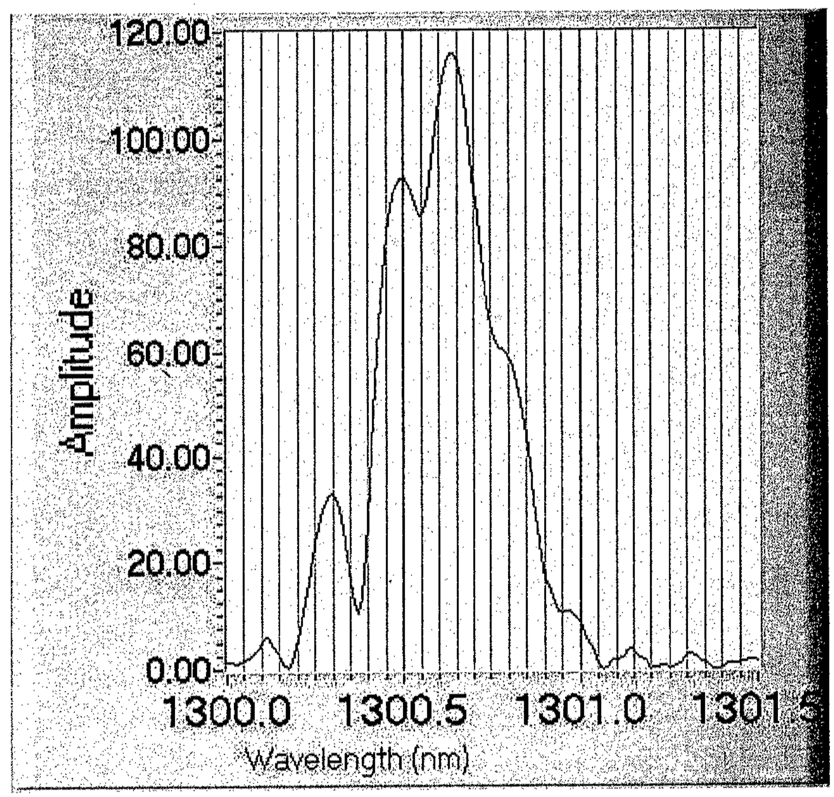

(b)

Spectral Profile of Sensor #4 (a) before and (b) after curing process

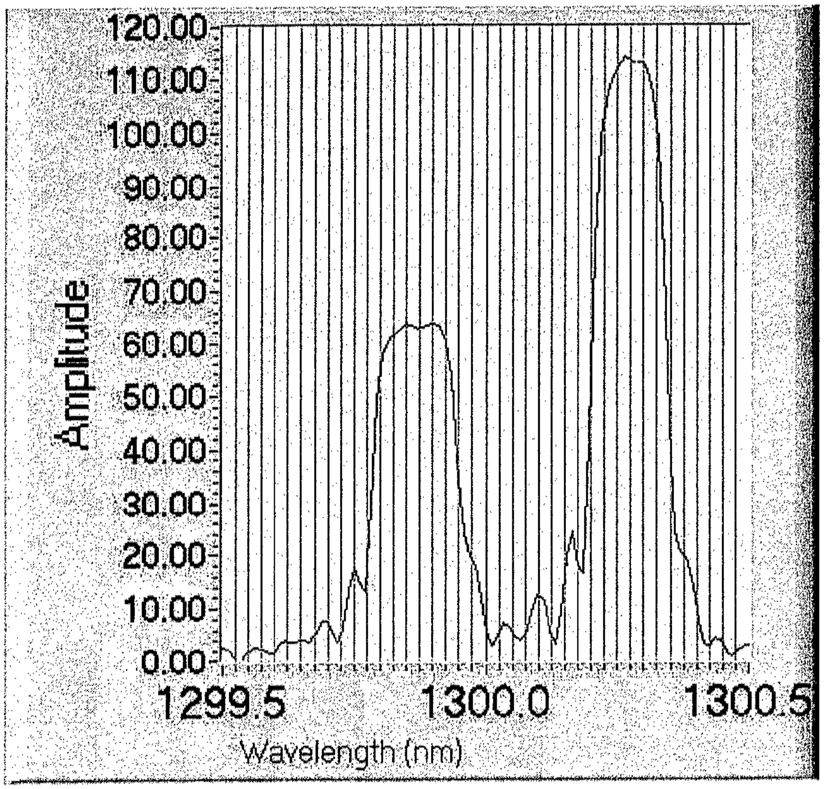

(a)

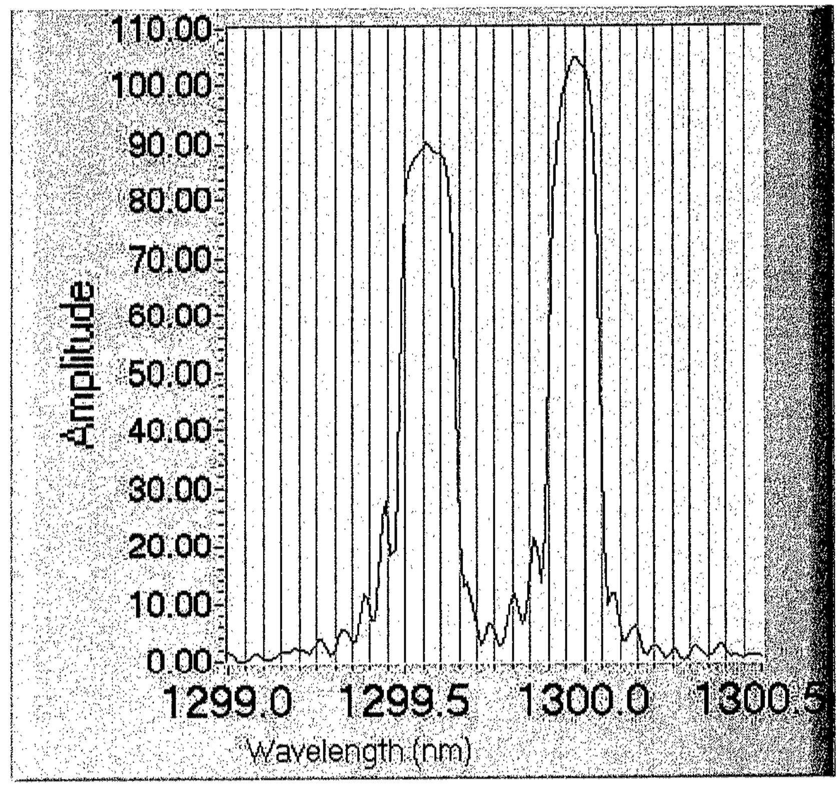

(b)

Spectral Profile of Sensor #8 (a) before and (b) after curing process

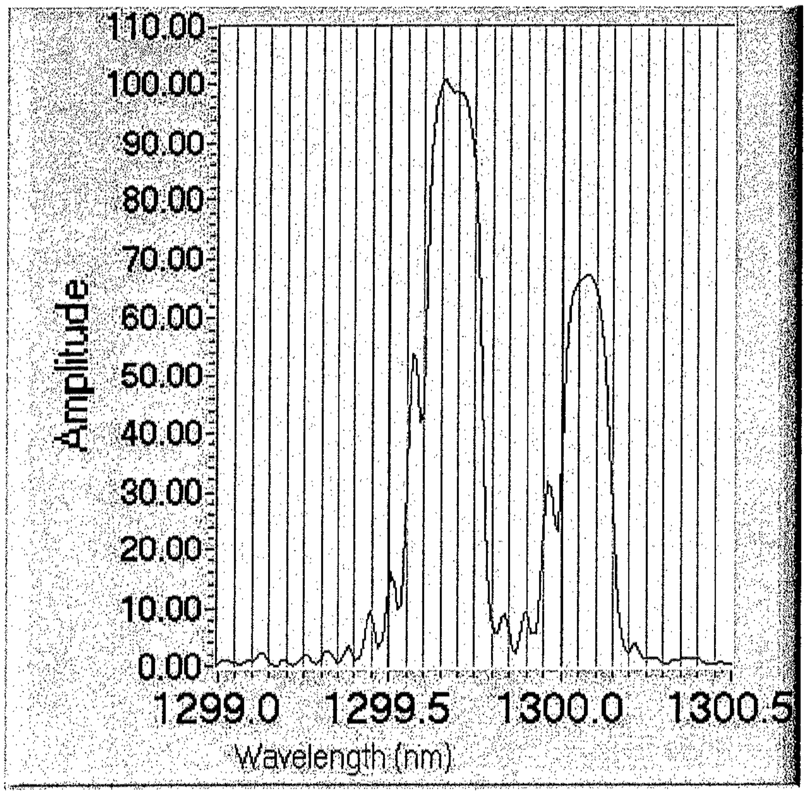

(a)

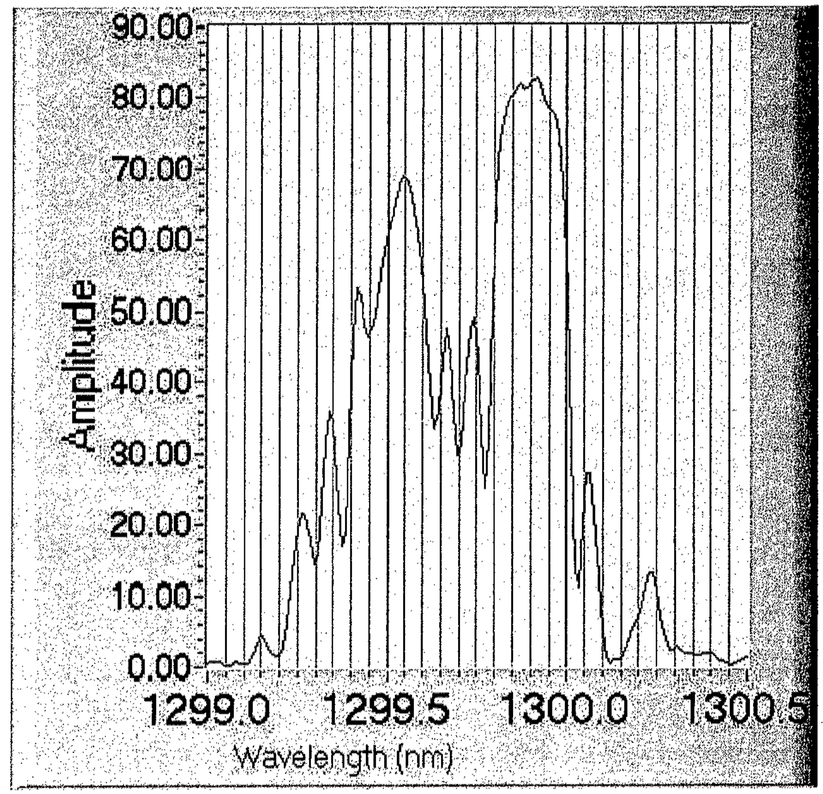

(b)

Sequence of Spectral Profiles from Sensor 2 Near Teflon Tape Damage Site during 1st pressure cycle

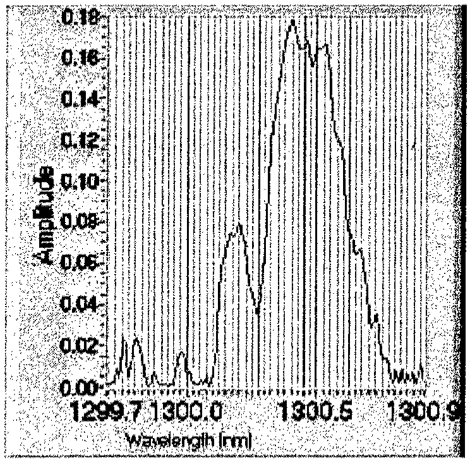

0 psi

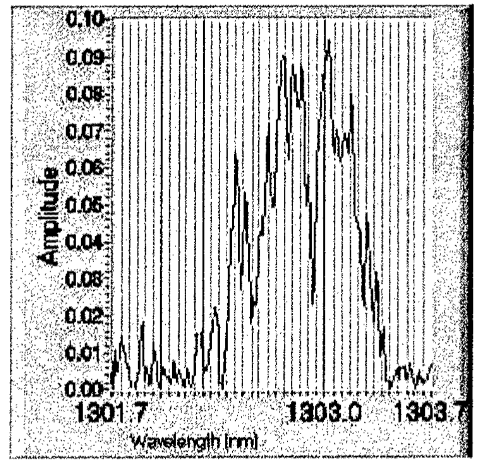

666 psi

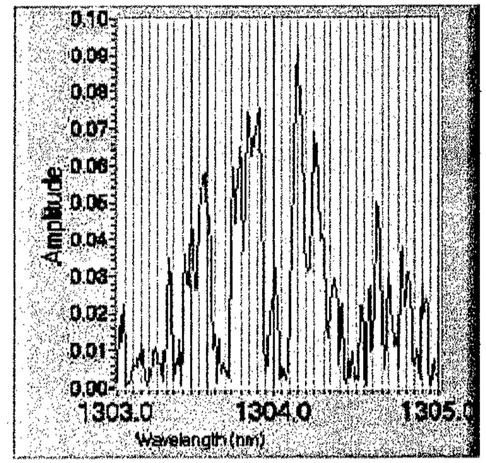

1000 psi

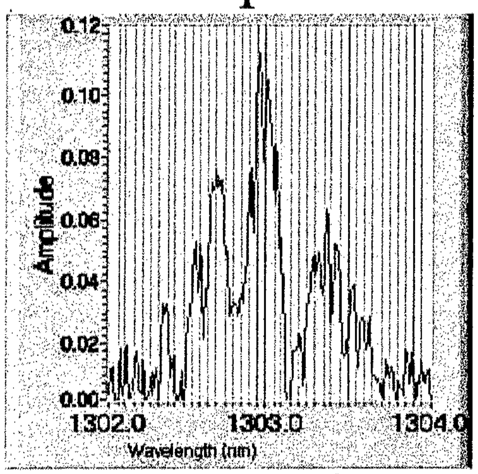

666 psi

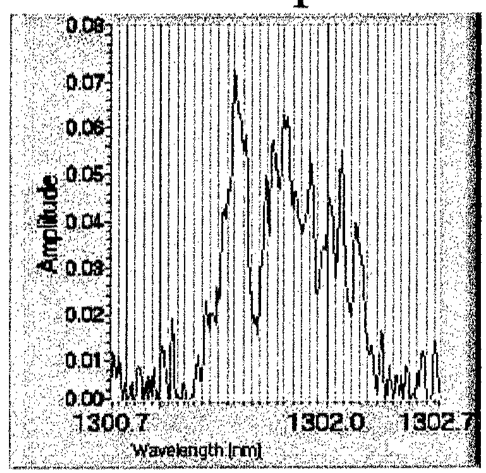

333 psi

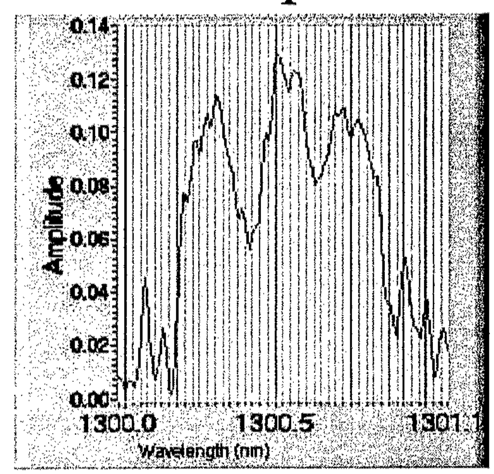

Return to 0 psi

BLUE ROAD RESEARCH

Spectral Profiles of Sensor 2 After Impact 3 Near Teflon Tape Area During 4th Pressure Cycle

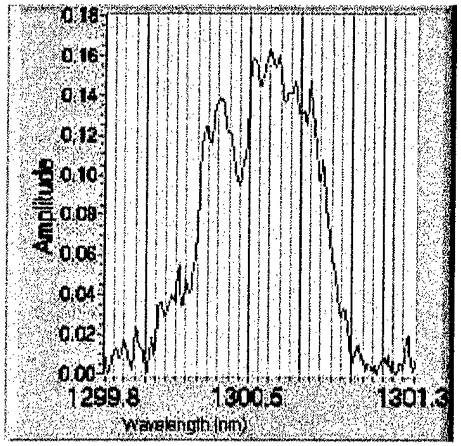

0 psi

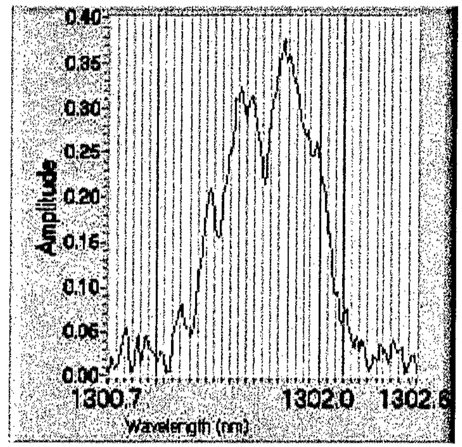

333 psi

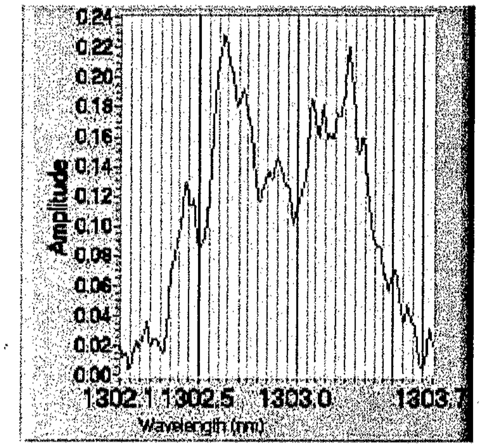

666 psi

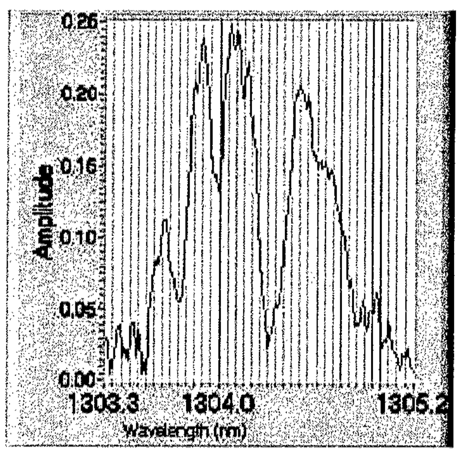

1000 psi

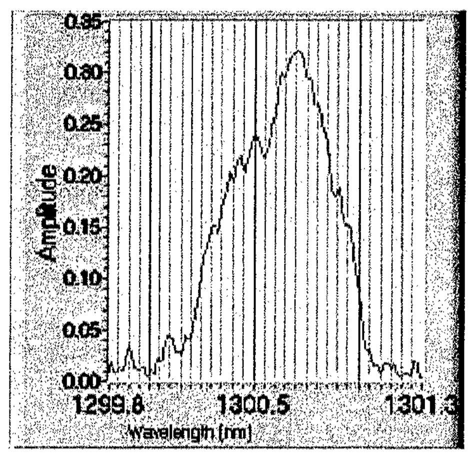

Return to 0 psi

Spectral Profiles of Sensor 4 After Impact 2 During 3rd Pressure Cycle Remote From Any Damage Site

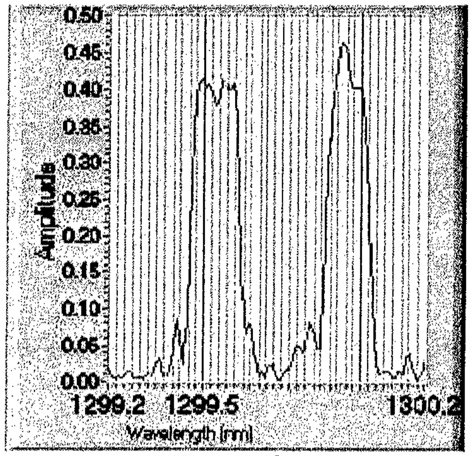

0 psi

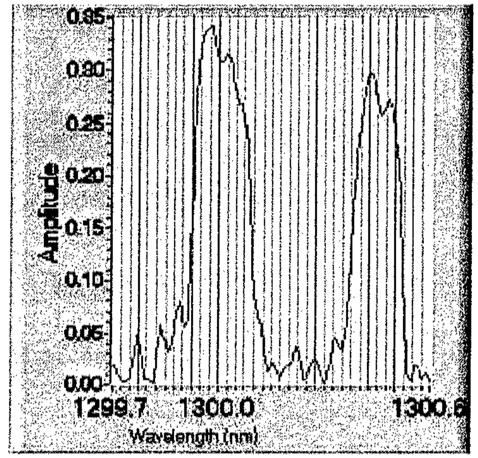

333 psi

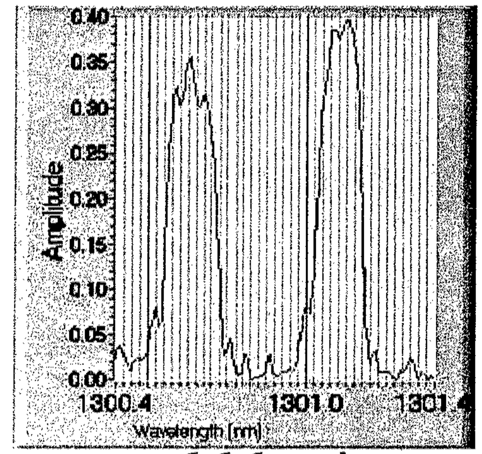

666 psi

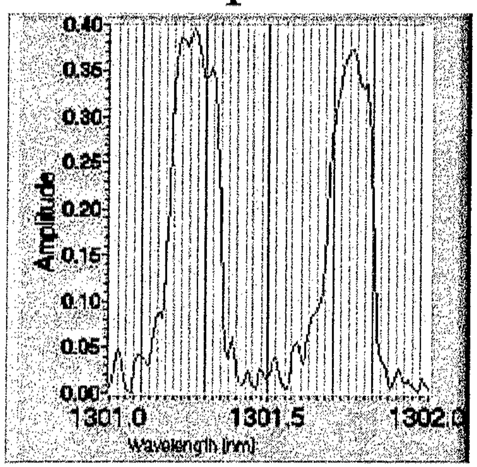

1000 psi

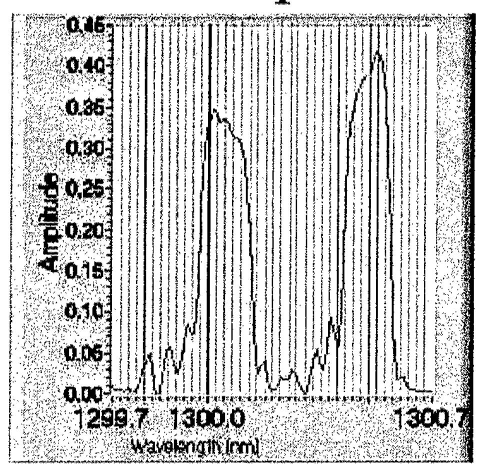

333 psi

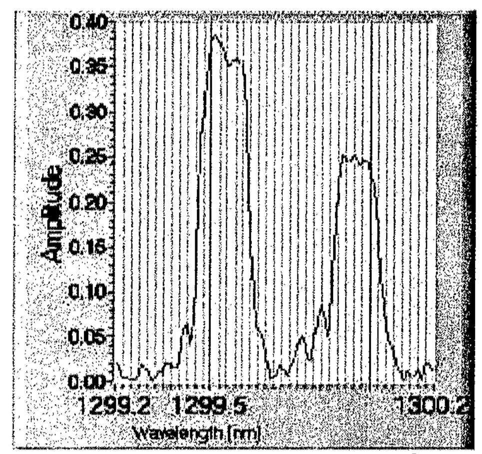

Return to 0 psi

BLUE ROAD RESEARCH

Spectral Profiles of Sensor 8 Near Cut Tow Area During 1st Pressure Cycle

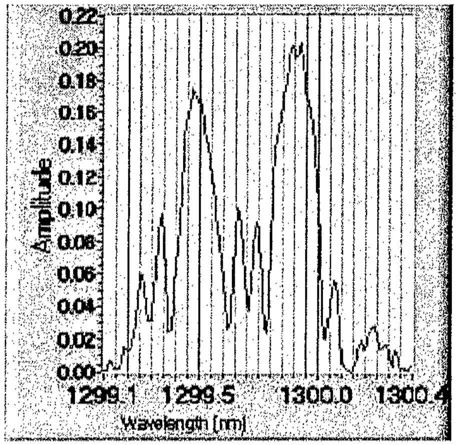

0 psi

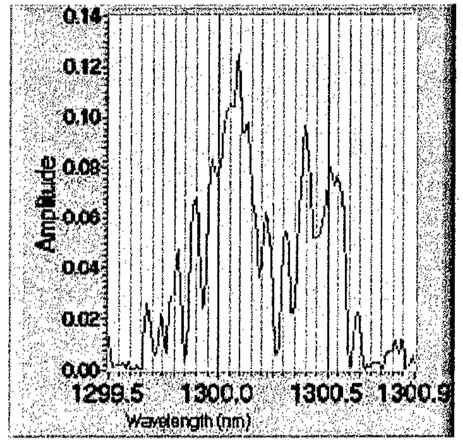

333 psi

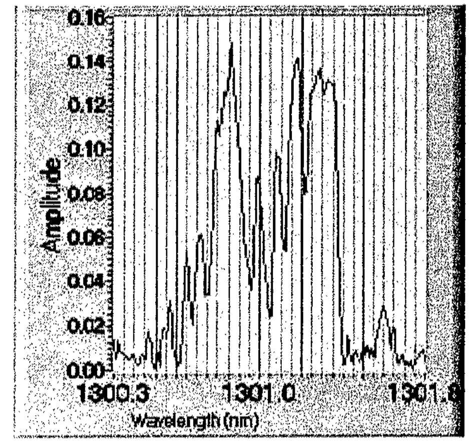

667 psi

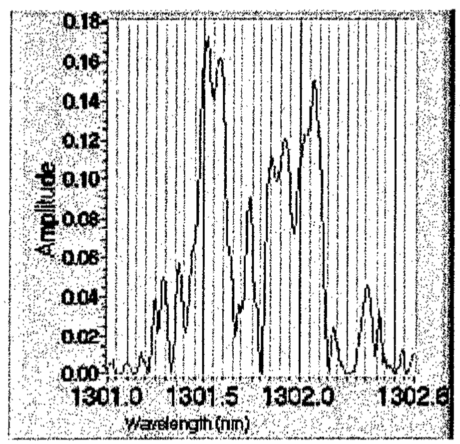

1000 psi

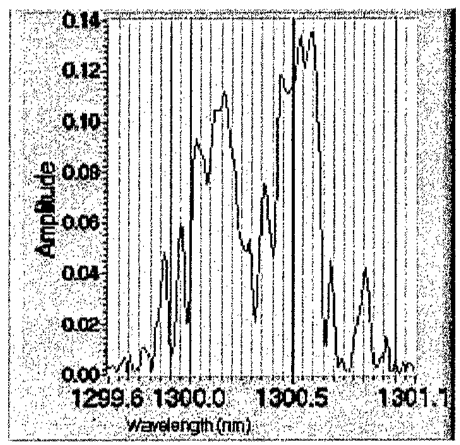

333 psi

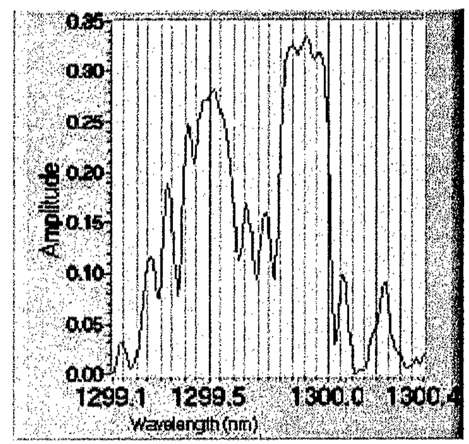

Return to 0 psi

BLUE ROAD RESEARCH

Spectral Profiles of Sensor 8 After Impact 2 Near Cut Tow Area During 3rd Pressure Cycle

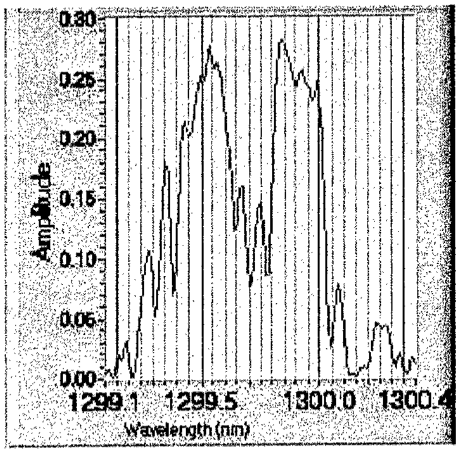

0 psi

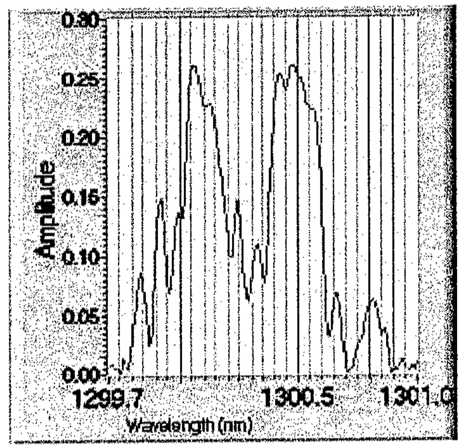

333 psi

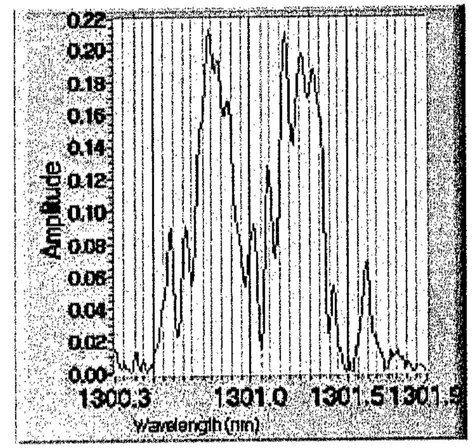

667 psi

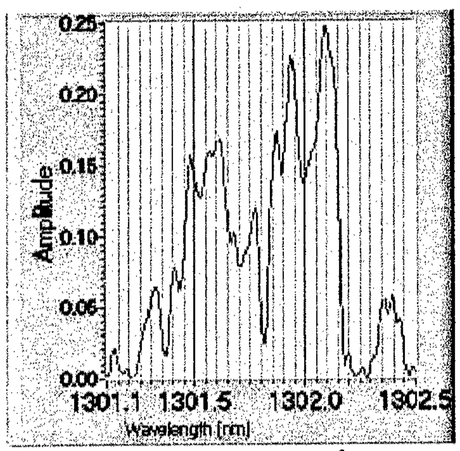

1000 psi

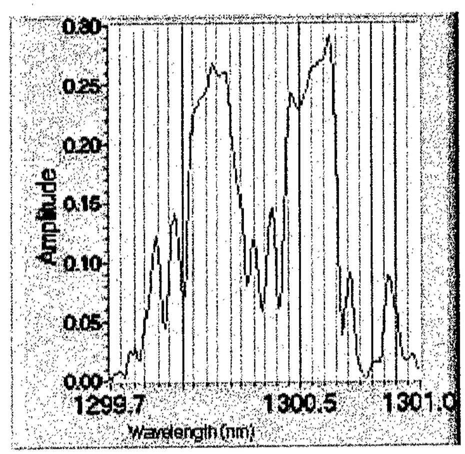

333 psi

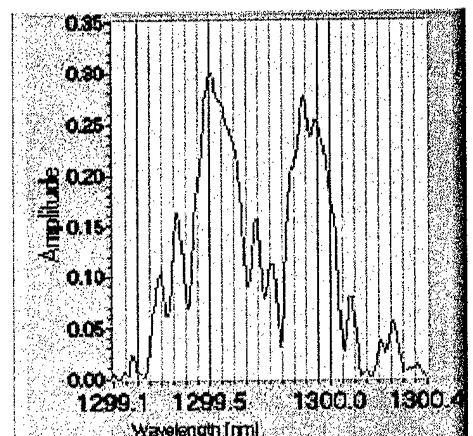

Return to 0 psi

BLUE ROAD RESEARCH

Drop Test Setup and Damage Induced

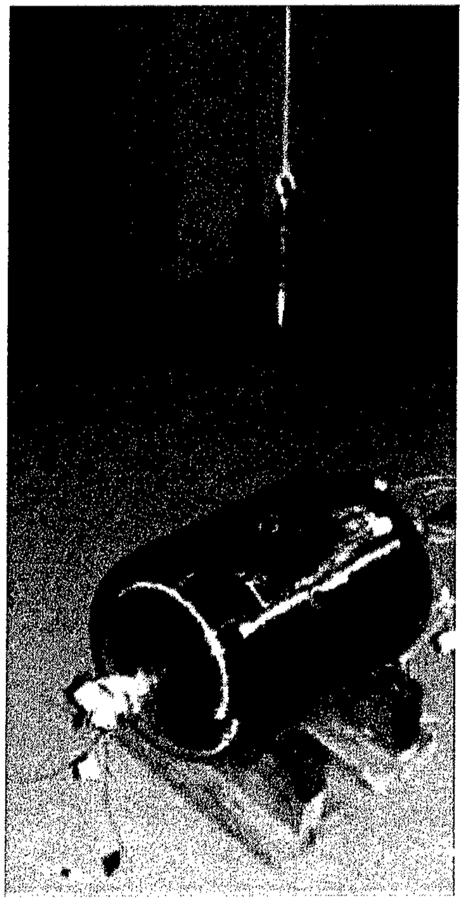

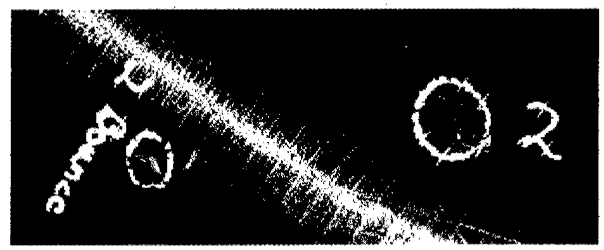

Damage induced by drop test 2 with bounce, 15 foot pound drop on 1 cm^2 area, ≈ 2.5 cm from sensors 7 and 8 near cut tow area

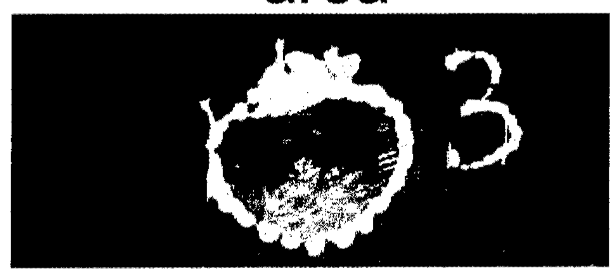

Drop test 3, a 30 foot pound drop on 1 cm^2 area ≈ 2.5 cm from sensors 1 and 2 near Teflon tape

BLUE ROAD RESEARCH

Cross Sectional View of Pressure Bottle Sensors and Impact Locations

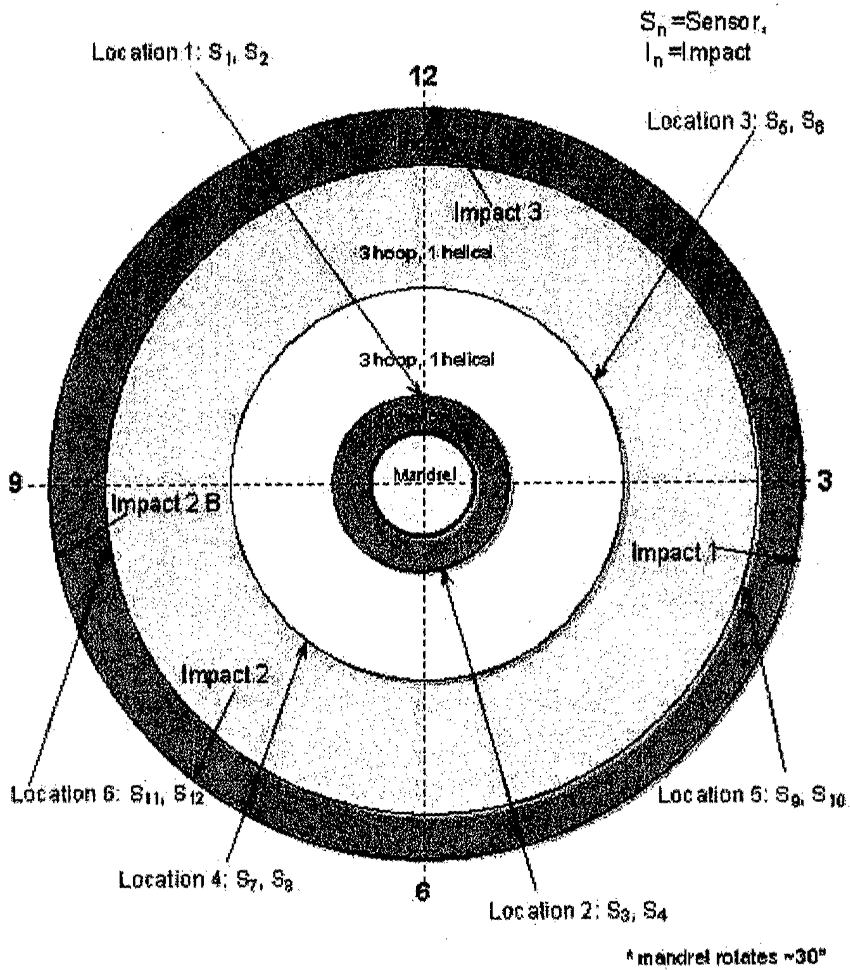

BLUE ROAD RESEARCH

5 ft-lb Impact, Near Sensor # 9

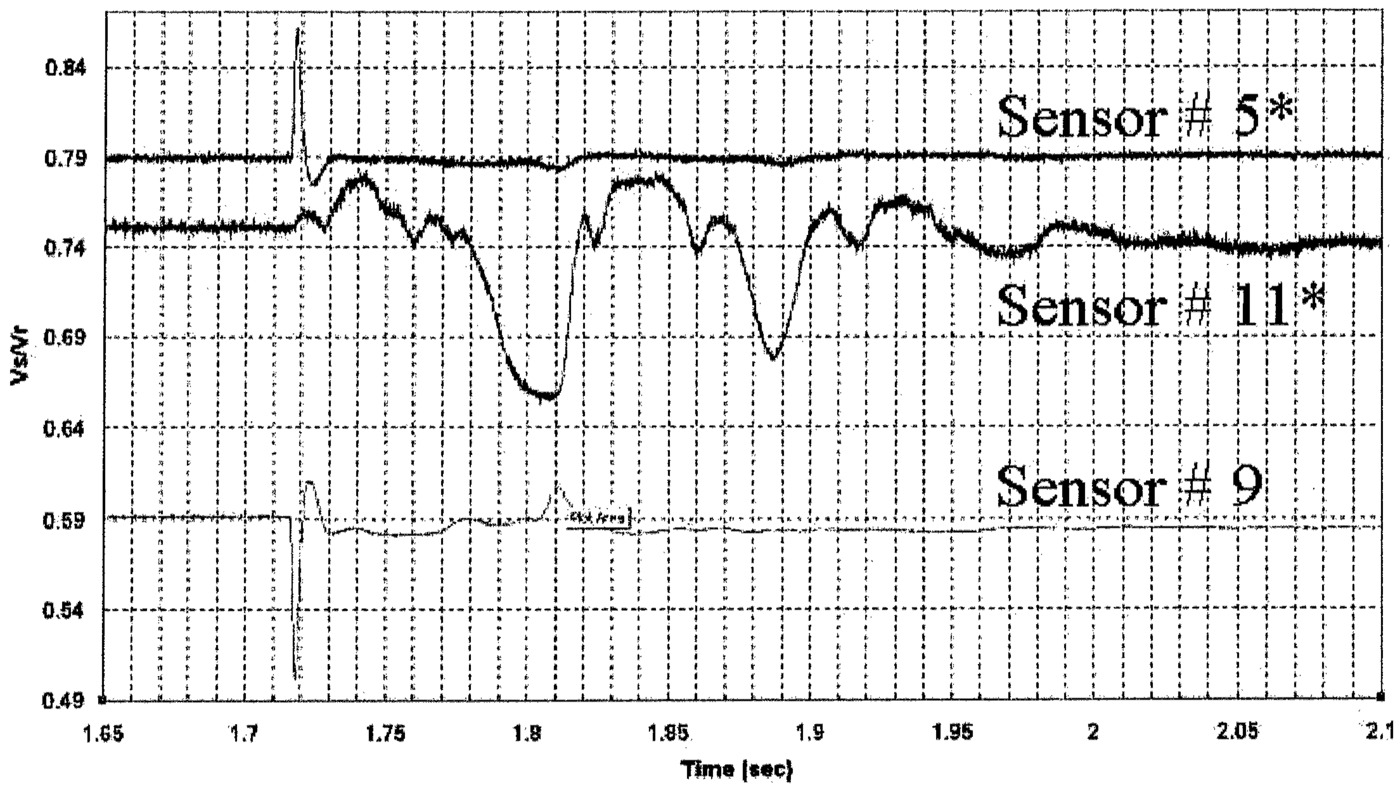

*Sensor 11 is in the top layer on the opposite side of the article from sensor 9, sensor 5 is in the middle layer in ≈ the same position as sensor 9

15 ft-lb Impact (and Bounce) Near Site of Cut Tow Damage and Sensor 7

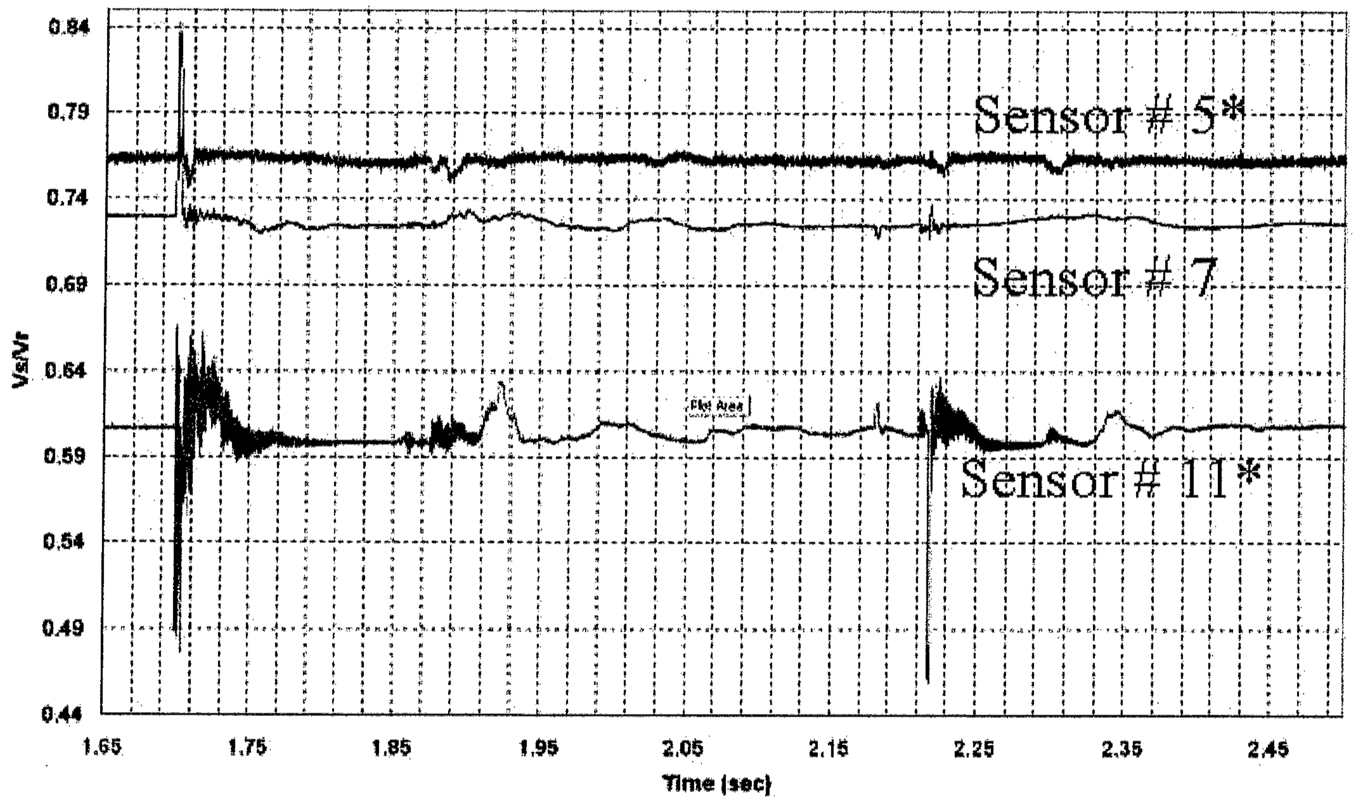

*Sensor 5 is located in the same middle layer as sensor 7 but on the opposite side of the tank. Sensor 11 is on the top layer on the same side of the tank as the impact/sensor 7

BLUE ROAD RESEARCH

Strain Measurements Made During 1st Pressure Cycle

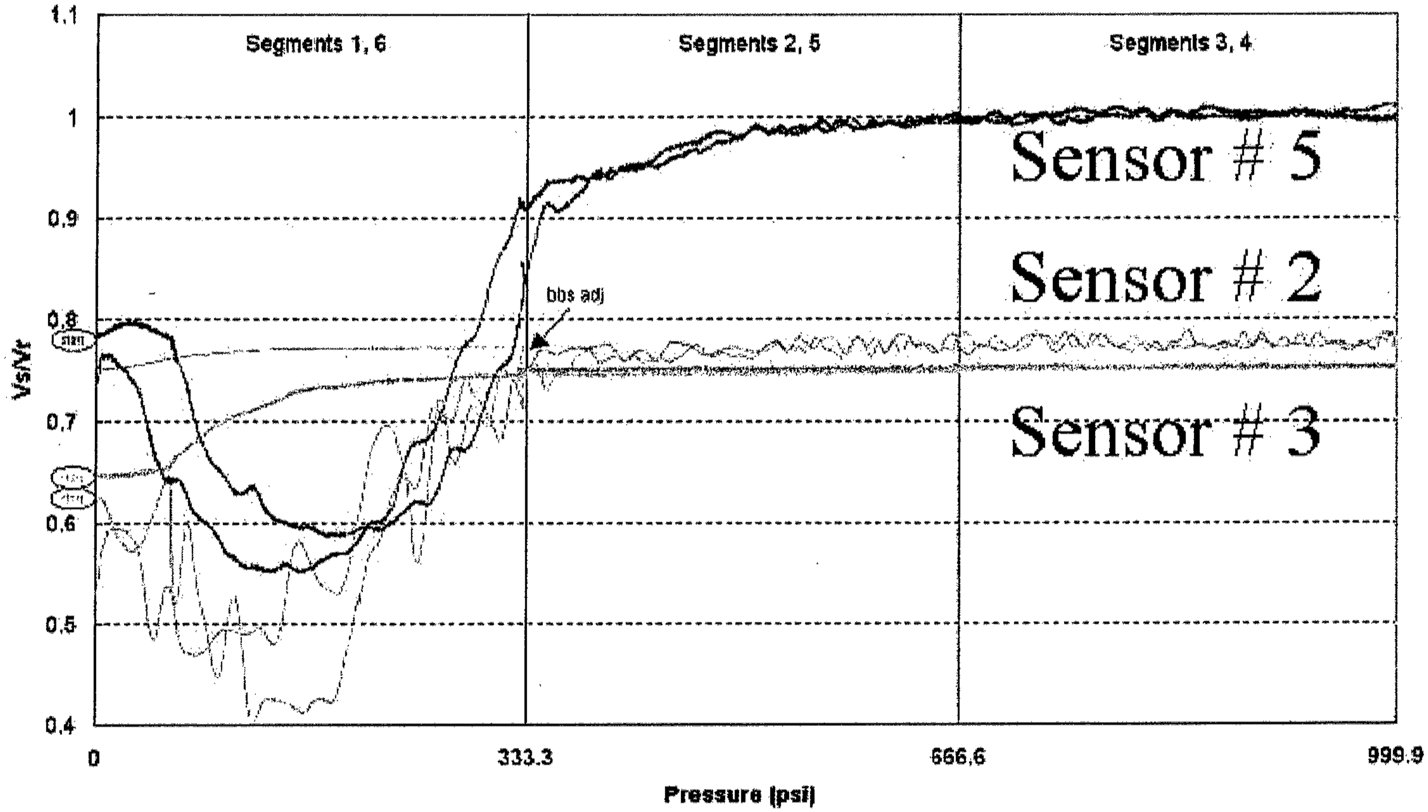

Sensor 2: deepest embedded layer, near Teflon tape flaw
Sensor 3: opposite side of tank, in same layer as sensor 2
Sensor 5: middle embedded layer in same area as sensor 2

BLUE ROAD RESEARCH

Pressure Cycle 3 After the 5 and 15 ft-lb Impacts

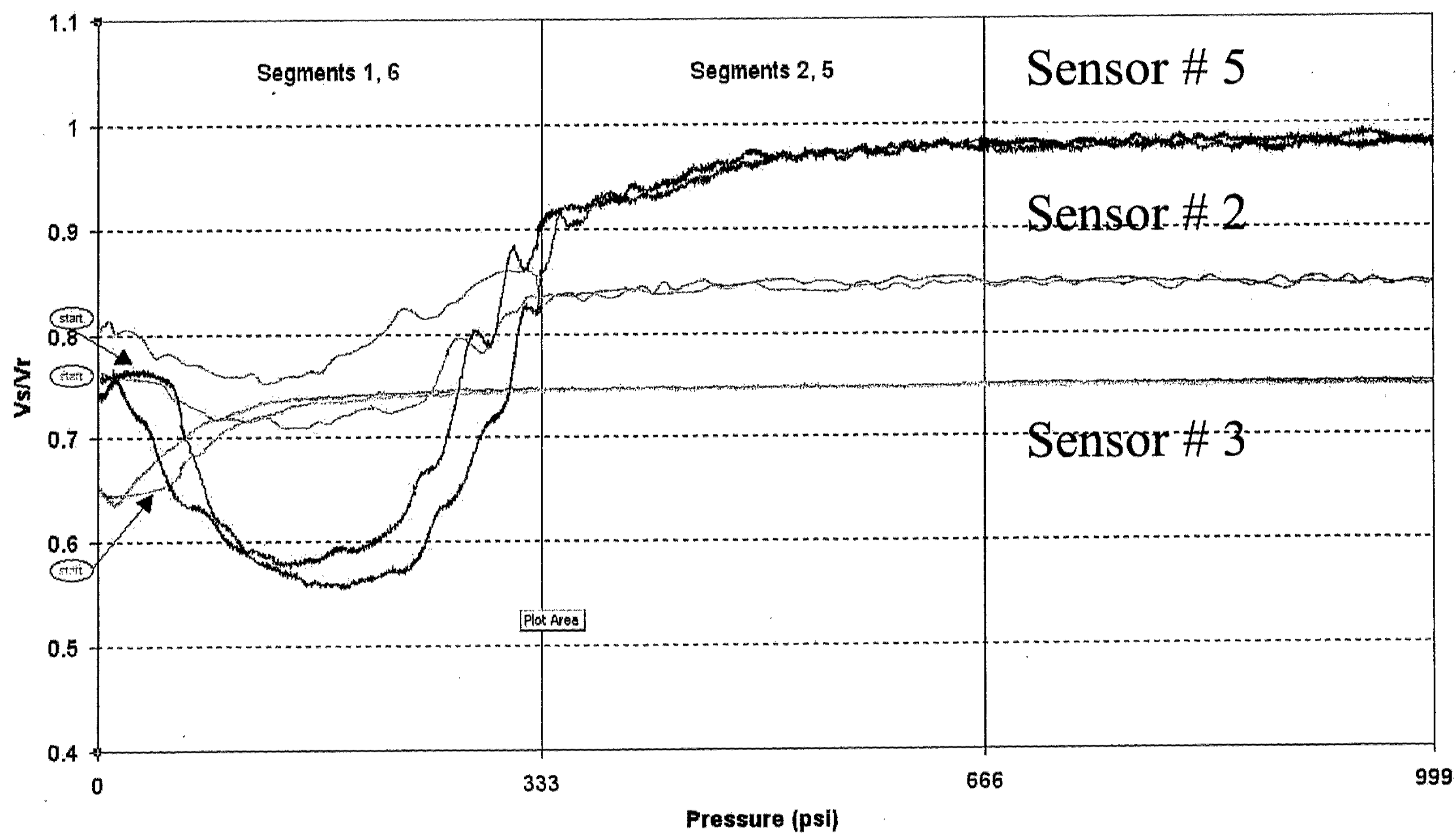

BLUE ROAD RESEARCH

Eddy Current Scan

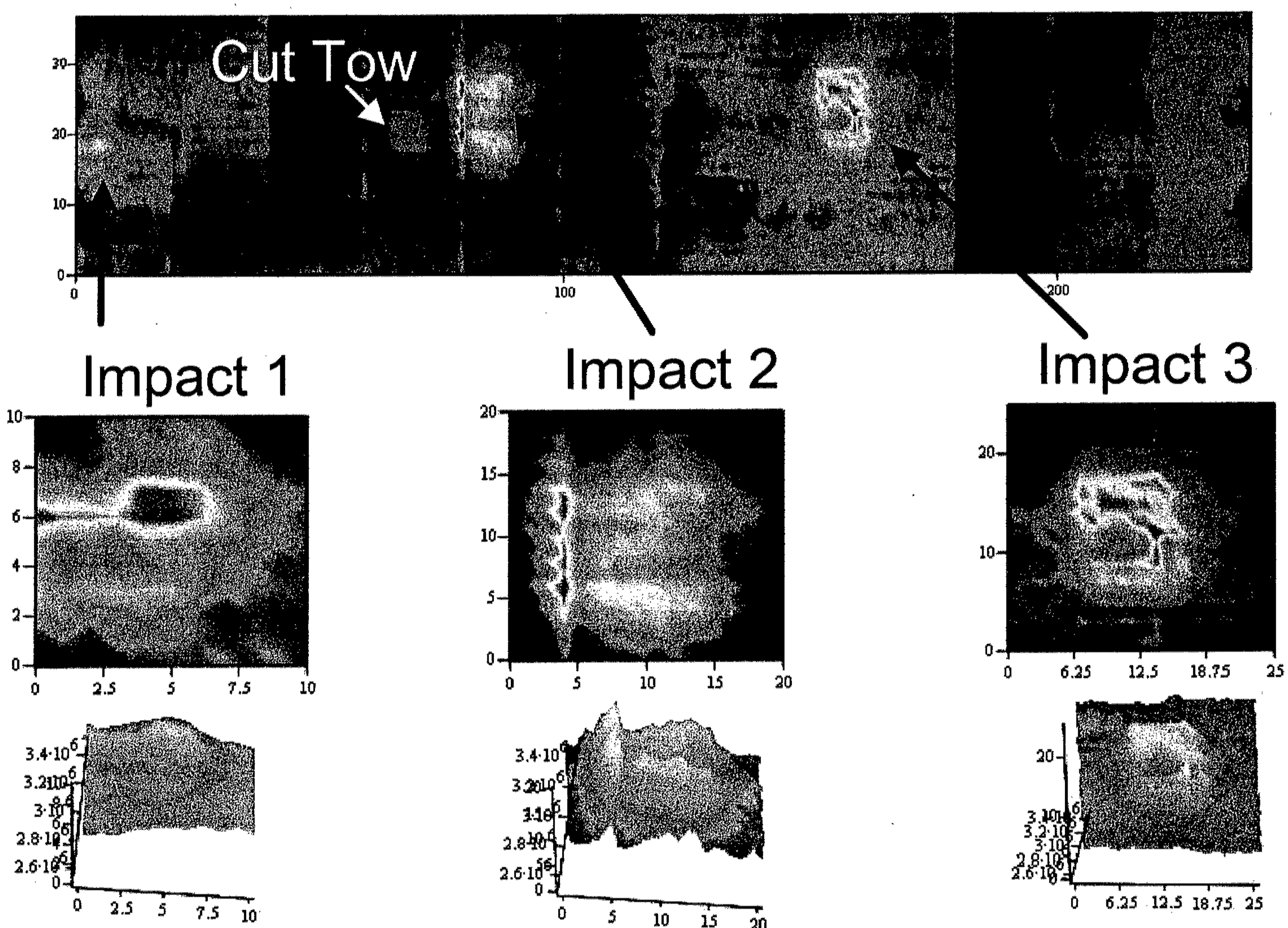

Summary

- Multi-axis fiber grating strain sensors can be used for quantitative damage assessment of adhesive joints

- Cut tow and Teflon tape defects may be detected using multi-axis fiber grating strain sensors

- Quantitative measurements of the evolution of damage due to pressure cycling and impacts can be made using multi-axis fiber grating strain sensors